universität wien

DIPLOMARBEIT / DIPLOMA THESIS

Titel der Diplomarbeit / Title of the Diploma Thesis

„The Effect of AP301 on the Expression of α- and δ-ENaC in A549 and RPMI-2650 cells“

verfasst von / submitted by

Martin Kraihammer

angestrebter akademischer Grad / in partial fulfilment of the requirements for the degree of

Magister der Pharmazie (Mag.pharm.)

Wien, 2015 / Vienna, 2015

Studienkennzahl lt. Studienblatt / degree programme code as it appears on the student record sheet:	A 449
Studienrichtung lt. Studienblatt / degree programme as it appears on the student record sheet:	Diplomstudium Pharmazie
Betreut von / Supervisor:	ao. Univ.-Prof. Mag. Dr. Rosa Lemmens

Table of contents

Acknowledgements

First and foremost, I would like to thank my supervisor Prof. Dr. Rosa Lemmens-Gruber for providing the possibility to carry out this research. Her guidance, patience and sustained encouragement as well as her keen eye for detail were essential for the success of this project. As a student, it is a privilege to have such a shrewd and experienced supervisor, who can always be approached for advice.

Furthermore, I owe special thanks to Dr. Waheed Shabbir and Dr. Mohammed Aufy, who imparted their vast knowledge on electrophysiology and biochemistry on me. Their perseverance and creativity enabled me to solve many problems along the way. Thank you for providing an enjoyable atmosphere, which encouraged scientific curiosity and discussion.

Not uncredited should go the valuable support by Pakiza Rawnduzi and Shahid Muhammad Iqbal, MSc. Thank you for answering countless questions, patiently explaining devices and procedures, and always having a sympathetic ear for a student in trouble.

I was fortunate to share the lab with many congenial students. Thank you for the lovely time together!

Of course, no acknowledgement can be complete without mentioning one's family. Above all, I would like to thank my parents for providing me with the possibility to pursue my dreams and to do what I enjoy. Special thanks also go to my sisters, who are an endless source of joy and happiness for me. I hold you all very dear.

In closing, I'd like to give a quote from one of my favourite writers, Bertrand Russell, whose ingenious books should be on everyone's bedside table:

"The good life is inspired by love and guided by knowledge."

Abstract

Das nichtkardiale Lungenödem ist eine lebensbedrohliche Erkrankung, die durch Akkumulation von extravasaler Flüssigkeit in der Lunge gekennzeichnet ist.

Da fortwährend Flüssigkeit von den pulmonalen Blutgefäßen in den Alveolarraum aufgrund des Blutdrucks gepresst wird, hat die Lunge Mechanismen entwickelt, um diese Flüssigkeit zu entfernen und so Atemnot vorzubeugen. Dieser Prozess, der als alveoläre Flüssigkeitsclearance (AFC) bezeichnet wird, wird durch vektoriellen Salz- und Wassertransport über das distale respiratorische Epithel getrieben. Der epitheliale Natriumkanal (ENaC) spielt eine bedeutende Rolle bei der alveolären Flüssigkeitsclearance, indem er den Eintritt von Na^+-Ionen an der apikalen Seite der alveolären Epithelzellen ermöglicht.

Bisher wurde, abgesehen von mechanischer Beatmung, noch keine Behandlungsmöglichkeit für Patienten mit nichtkardialem Lungenödem gefunden.

AP301, ein cyclisches Peptid, das die Lektin-ähnliche Domäne (genannt TIP-Domäne) von Tumornekrosefaktor alpha (TNF-α) imitiert, wird zurzeit in klinischen Studien für diese Indikation geprüft. Erst kürzlich hat dieser Wirkstoff Phase I und IIa abgeschlossen. Bisher veröffentlichte Daten aus Patch-Clamp-Experimenten zeigen, dass AP301 in der Lage ist ENaC *in vitro* zu aktivieren. Diese Wirkung wird zum Teil über direkte Aktivierung des Kanals durch Bindung von AP301 an ENaC ausgelöst. Jedoch ist noch unklar, ob AP301 auch die Proteinexpression von ENaC beeinflusst, womit die in Patch-Clamp-Versuchen beobachtete Steigerung von Na^+-Strömen ebenfalls erklärt werden könnte.

Diese Arbeit wurde durchgeführt, um zu erforschen, ob die Expression der porenbildenden ENaC-Untereinheiten α und δ in Zellkulturen durch Behandlung mit AP301 beeinflusst wird. Zwei Zelllinien, die ENaC endogen exprimieren wurden verwendet: Die Adenocarcinom-Zelllinie A549 mit alveolärem Phänotyp und die nasale epitheliale Zelllinie RPMI-2650. cDNA von teils oder vollständig unglykosylierten α-hENaC-Mutanten wurde heterolog in HEK-293 Zellen exprimiert, um die Bedeutung der Glykosylierung auf die Wirkung von AP301 zu erforschen. Mithilfe der Western Blot-Technik wurden Zelllysate untersucht, um die Expressionsniveaus von ENaC abschätzen zu können.

Die Resultate dieser Arbeit zeigen, dass die Expression von α- und δ-ENaC in A549 und α-ENaC in RPMI-2650 Zellen, die mit AP301 behandelt wurden, wahrscheinlich transient hochreguliert wird. Allerdings war die statistische Signifikanz bei diesen Experimenten gering. Bei unglykosylierten α-hENaC-Mutanten, die in HEK-293 Zellen exprimiert wurden, bleibt diese Wirkung aus. Dieses Ergebnis hebt die Bedeutung der Glykosylierung für die Wirkung von AP301 auf ENaC hervor.

Schlüsselwörter: Lungenödem, ENaC, Glykosylierung, TNF-α, AP301, Western Blot

Abstract

Non-cardiogenic pulmonary edema is a life-threatening condition characterized by accumulation of extravascular fluid in the lung.

Since fluid is constantly forced from the pulmonary blood vessels into the alveolar space due to blood pressure, the lung has evolved mechanisms to remove this liquid in order to avoid respiratory distress. This process called alveolar fluid clearance (AFC) is driven by vectorial salt and water transport across the distal pulmonary epithelium. The epithelial Na^+ channel (ENaC) plays a major role in AFC, facilitating Na^+ entry at the apical side of alveolar epithelial cells.

Apart from mechanical ventilation, no specific treatment for non-cardiogenic pulmonary exists so far.

AP301, a cyclic peptide mimicking the lectin-like domain (termed TIP domain) of tumor necrosis factor alpha (TNF-α), is currently evaluated in a clinical setting for this indication, having recently completed phase I and IIa trials. Previously published data from patch-clamp studies shows that AP301 is capable of activating ENaC *in vitro*. This effect is in part mediated by direct channel activation through binding of AP301 to ENaC. However, it is still unclear if AP301 also influences protein expression of ENaC, which could also account for an increase in Na^+ currents observed in patch-clamp experiments.

This study was undertaken to determine whether expression of the pore-forming ENaC subunits α and δ is altered in cell cultures through treatment with AP301. Two cell lines expressing ENaC endogenously were used: the adenocarcinomic cell line A549 with an alveolar type II cell phenotype and the nasal epithelial cell line RPMI-2650. cDNA of partly or completely unglycosylated α-hENaC mutants was expressed heterologously in HEK-293 cells to examine the importance of glycosylation on the effect of AP301. Western blotting was performed on cell lysates to estimate ENaC expression levels in these cells.

The results of this study show that α- and δ-ENaC expression is probably transiently upregulated in A549 treated with AP301, whereas increased expression in RMPI-2650 cells was only appreciable for α-ENaC. However, statistical significance for these experiments was poor. No effect could be observed on unglycosylated α-hENaC mutants expressed in HEK-293 cell. This finding highlights the importance of glycosylation for the effect of AP301 on ENaC.

Keywords: pulmonary edema, ENaC, glycosylation, TNF-α, AP301, Western blot

List of Abbreviations

AFC	Alveolar fluid clearance
ALI	Acute lung injury
AQP	Aquaporin
ARDS	Acute respiratory distress syndrome
ASIC, cASIC	Acid-sensing ion channel, chicken ASIC
AT1 cells	Alveolar type I cells
AT2 cells	Alveolar type II cells
CAP	Channel activating protease
CFTR	Cystic fibrosis transmembrane conductance regulator
CHO cells	Chinese hamster ovary cells
CNGC, CNG channel	Cyclic nucleotide-gated channel
DEG	Degenerin
DMEM/F-12	Dulbecco's modified Eagle medium/F12 nutrient mixture Ham + L-Glutamine
ECL	Enhanced chemiluminescence
EMA	European Medicines Agency
FBS	Fetal bovine serum
GFP	Green fluorescent protein
HEK-293 cells	Human embryonal kidney 293 cells
hENaC	Human epithelial sodium (Na^+) channel
HSC	Highly selective cation channel
MARCKS	Myristoylated alanine-rich C-kinase substrate
Nedd4-2	neural precursor cell expressed developmentally down-regulated protein 4-2

NSC	Non-selective cation channel
PBS	Phosphate buffered saline
PIP_2	Phosphatidylinositol 4,5-bisphosphate
PNGase F	peptide-N4-(N-acetyl-β-D-glucosaminyl)asparagine amidase
PVDF	Polyvinylidene difluoride
SDS-PAGE	Sodium dodecyl sulfate – polyacrylamide gel elektrophoresis
TBS	Tris-buffered saline
TEMED	Tetramethylethylenediamine
TIP domain	Lectin-like domain of TNF-α
TNF-α	Tumor necrosis factor alpha
WT	Wild type

List of Figures

List of Tables

1. Introduction

1.1. Epithelial sodium channel (ENaC)

The epithelial sodium (Na^+) channel is a pore-forming transmembrane protein, which is highly permeable for Na^+ and Li^+ ions as well as protons, but shows a very small conductance for other cations like K^+ (Palmer, 1987). Unlike voltage-gated Na^+ channels of muscle and neurons, ENaC is voltage-independent and constitutively active (Snyder, 2002). Horisberger and Chraïbi argue that ENaC may be classified as a ligand-gated ion channel (Horisberger and Chraïbi, 2004).

ENaC is part of the DEG/ENaC superfamily of ion channels, which was termed based on the names of the first two identified subfamilies (Mano and Driscoll, 1999). Members of this family of ion channels are expressed in a variety of tissues in the mammalian body and have also been identified in other species, including the nematode *Caenorhabditis elegans*, the common fruit fly *Drosophila melanogaster* and species of marine snails (Mano and Driscoll, 1999; Kashlan and Kleyman, 2011; Kellenberger and Schild, 2014).

Like all the other members of the DEG/ENaC superfamily which have been examined, ENaC is highly sensitive to the K^+-sparing diuretic amiloride (Garty, 1994; Schild et al., 1997; Kashlan and Kleyman, 2011).

1.1.1. Structure

1.1.1.1. Subunits

In epithelial cells, ENaC is comprised of three homologous subunits named α-, β- and γ-ENaC (Canessa et al., 1994b). A fourth subunit termed δ-ENaC was found, which shows similar conductance properties to the α subunit (Waldmann et al., 1995). These subunits share about 30-35% sequence identity (Waldmann et al., 1995; Snyder, 2002).

α- and δ-ENaC seem to act as the pore-forming subunits and produce small ion currents even when expressed alone (Waldmann et al., 1995). However, for maximal efficient expression of the channel co-expression of β- and γ-ENaC is required (Canessa et al., 1994b; McDonald et al., 1995; Firsov et al., 1996).

The four subunits share a common structure of two membrane-spanning α-helical domains, connected by a large extracellular loop and short intracellular N- and C-terminal regions (Fig. 1) (Canessa et al., 1994a; Renard et al., 1994; Snyder et al., 1994). The extracellular region constitutes approximately 70% of the mass of each ENaC subunit (Kashlan and Kleyman, 2011), in part owing to numerous glycosylation sites, the exact number of glycosylated residues varying between subunits (Prince and Welsh, 1998; Valentijn et al., 1998).

1.1.1.2. Channel stoichiometry

To date the exact stoichiometry of ENaC remains uncertain. Over the last two decades, various research groups tried to unravel this mystery using different approaches: Functional and biochemical evidence as well as freeze-fracture electron microscopy and fluorescence resonance energy transfer studies suggested a complex of either four [α2βγ] (Firsov et al., 1998; Kosari et al., 1998) or nine subunits [α3β3γ3] (Snyder et al., 1998; Eskandari et al., 1999; Staruschenko et al., 2004, 2005).

The recently published structure of the chicken acid-sensing ion channel 1 at 1.9 Å helped resolve this issue (Jasti et al., 2007). Based on the structural properties of this closely related protein of the ENaC/degenerin superfamily, a heterotrimeric complex [αβγ] for ENaC seems very likely (Kashlan and Kleyman, 2011). Recent results from an atomic force microscopy study confirm this heterotrimeric structure and also provide evidence for potential formation of homotrimers as well as higher-order structures containing two or three trimers, which would account for former results (Stewart et al., 2011).

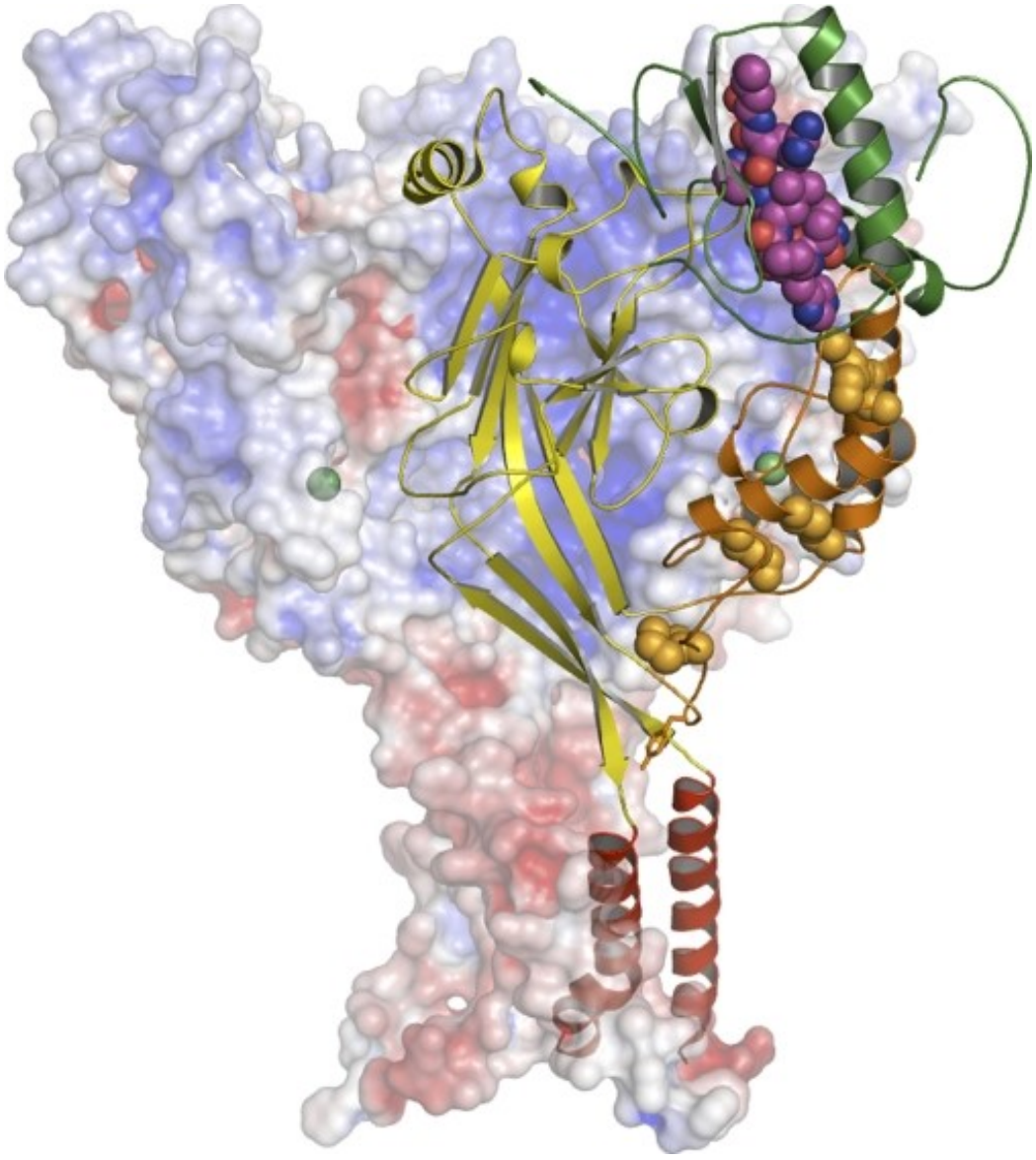

Fig. 1. Model of α-ENaC, shown as a homotrimer. One subunit is represented as a ribbon. The other two subunits are depicted as a surface with relatively acidic (red) and basic (blue) areas indicated. The large extracellular loop of α-ENaC is probably comprised of five distinct domains and vaguely resembles an outstretched hand: Palm and β-ball are antiparallel β-sheets possibly located in the core of the channel. The outer domains are termed knuckle, finger and thumb. These regions show lower sequence identity between ENaC subunits and ASIC1 and are seemingly modular. Different domains are colour-coded: red, transmembrane helices; yellow, palm, β-ball and knuckle; green, finger; orange, thumb. Orange spheres depict cysteine residues, forming five disulfide bonds. Possible binding sites for Cl^- ions, which modulate channel activity, are shown as green spheres. Eight residues of the inhibitory tract essential for peptide inhibition are represented by purple spheres (see 1.1.3.2. Proteolytic cleavage) (Kashlan and Kleyman, 2011).

1.1.2. Physiological role and location

ENaC plays a major role in Na^+ homeostasis in the human body controlling extracellular fluid volume and blood pressure, airway surface liquid volume and mucociliary clearance (Kashlan and Kleyman, 2011).

Palmer and Frindt first discovered an amiloride-sensitive Na^+-permeable ion channel in patch-clamp studies of rat cortical collecting tubules (Palmer and Frindt, 1986). This epithelial sodium channel was later found to be the main pathway for sodium reabsorption in the kidney, facilitating sodium transport across the apical membrane of epithelial cells (Garty, 1994). Sodium is subsequently removed from these cells by the Na^+/K^+-ATPase enzyme, located at the basolateral membrane, into the adjacent blood vessels (Rossier et al., 2002).

A similar process, involving these two proteins, is responsible for clearing liquid from the airspaces of the lung at birth and regulating lung fluid balance, including removal of excess fluid in case of pulmonary edema, in humans (Matthay et al., 2002).

α-, β- and γ-ENaC are expressed throughout the human body, including the kidneys, lung, colon and salivary glands, whereas δ-ENaC can be found in the ovaries, testis, pancreas and brain (Kellenberger and Schild, 2014). The physiological role of δ-ENaC, which to date has only been found in humans, is still unclear (Kellenberger and Schild, 2014).

1.1.3. Regulation of ENaC

Due to its vital role, ENaC is tightly regulated in the human body. A large number of regulation mechanisms have been elucidated in the last two decades, changing either channel open probability or the amount of ion channels expressed at the cell surface (Snyder, 2002).

1.1.3.1. Hormonal regulation

The main regulator of ENaC is the mineralocorticoid aldosterone, which is secreted by the adrenal gland in response to low plasma volume or increased plasma $[K^+]$ (Palmer et al., 2012). Aldosterone increases channel expression by inhibiting ubiquitylation and subsequent proteasomal degradation through a signalling cascade involving the E3 ubiquitin ligase Nedd4-2 (Schild, 2010).

Thus, aldosterone enhances Na^+ absorption in the kidney collecting duct and distal colon, raising plasma $[Na^+]$ and volume (Snyder, 2002).

Other hormonal regulatory factors of ENaC include vasopressin and glucocorticoids, which show similar effects to aldosterone (Snyder, 2005).

1.1.3.2. Proteolytic cleavage

Rather uncommon for an ion channel, ENaC can be activated by proteolytic cleavage (Kashlan et al., 2011). Vallet et al. provided the first evidence that serine proteases are capable of activating ENaC (Vallet et al., 1997). Subsequently, numerous soluble and membrane-bound proteases were identified, which stimulate ENaC activity, including trypsin, furin, elastase, kallikrein and the channel activating proteases prostasin (CAP1), CAP2 and matriptase (CAP3) (Kleyman et al., 2009; Kellenberger and Schild, 2014).

Proteolytic cleavage only increases channel open probability, without affecting ion selectivity or single-channel conductance (Chraïbi et al., 1998; Caldwell, 2003).

Proteolysis occurs in the finger domains of α- and γ-ENaC (Fig. 2), where cleavage by furin and prostasin in two positions and subsequent removal of the intervening inhibitory tracts activates the channel (Bruns et al., 2006; Carattino et al., 2006).

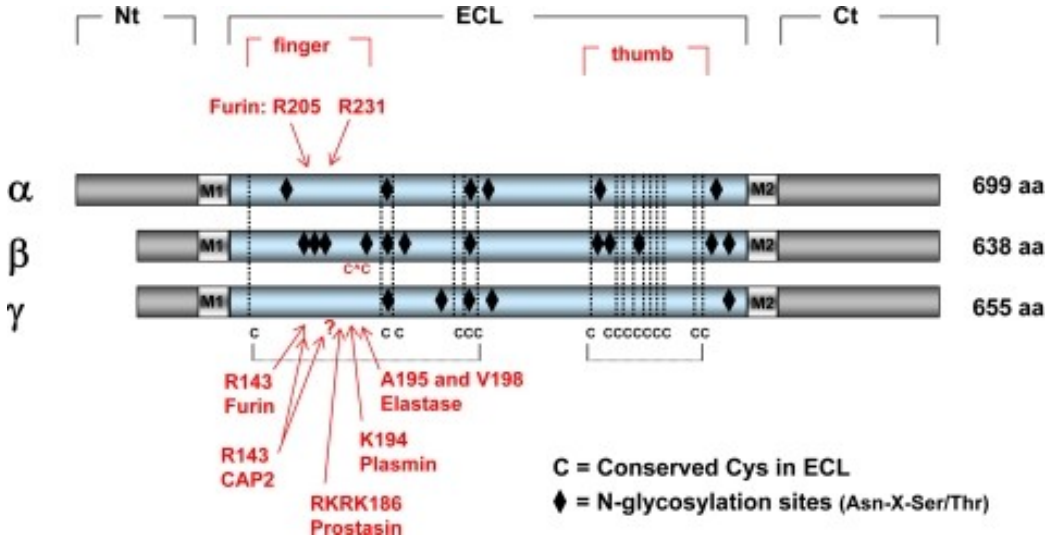

Fig. 2. Linear models of the ENaC subunits. Proteolytic cleavage of α- and γ-ENaC occurs in the large extracellular loop (ECL). Cleavage sites for furin, elastase, plasmin, prostasin (CAP1) and CAP2 are located within the finger domains in the extracellular regions. α-ENaC is cleaved twice by furin, whereas γ-ENaC has only one cleavage site for furin. β-ENaC lacks the consensus motifs for protease recognition and is therefore not processed. *aa*, amino acids; *C*t, C-terminal region, *Nt*, N-terminal region. (Kleyman et al., 2009).

1.1.3.3. Ions and mechanical stress

Extracellular and intracellular Na^+ concentrations regulate ENaC currents (Kashlan and Kleyman, 2011). A process known as Na^+ feedback inhibition is responsible for rapidly decreased ENaC activity in the face of elevated extracellular Na^+ concentrations (Horisberger and Chraïbi, 2004; Bize and Horisberger, 2007). Increased cytosolic Na^+ concentrations cause so-called Na^+ self-inhibition, a mechanism which reduces ENaC open probability and expression (Anantharam et al., 2006).

A variety of other factors modulate ENaC activity: increased renal tubular flow enhances ENaC open probability (Morimoto, 2006), extracellular protons increase Na^+ current probably by relieving Na^+ self-inhibition (Collier and Snyder, 2009a), whereas extracellular Cl^- ions inhibit ENaC activity (Collier and Snyder, 2009b).

1.1.3.4. Tumor necrosis factor alpha

For tumor necrosis factor alpha (TNF-α) a dichotomal role in ENaC regulation has been reported (Braun et al., 2005). TNF-α can decrease ENaC activity and expression levels via binding to the TNF receptor (Dagenais, 2004; Yamagata et al., 2009). On the other hand, the lectin-like domain of TNF-α was found to increase amiloride-sensitive currents across alveolar epithelial cells (Fukuda et al., 2001; Elia et al., 2003).

1.2. Acid-sensing ion channels (ASICs)

Acid-sensing ion channels are permeable to cations and are activated by extracellular acidosis (Wemmie et al., 2013). Like ENaC, ASICs are part of the DEG/ENaC superfamily and share a common topology (Fig. 3) (Mano and Driscoll, 1999). Recently published X-ray structures of ASIC helped clarify the structural properties of this superfamily of ion channels (Jasti et al., 2007; Baconguis et al., 2014).

ASICs are primarily expressed in the nervous system, where they are implicated in pain sensation, synaptic plasticity, expression of fear, and neurodegeneration after ischemia (Kellenberger and Schild, 2014).

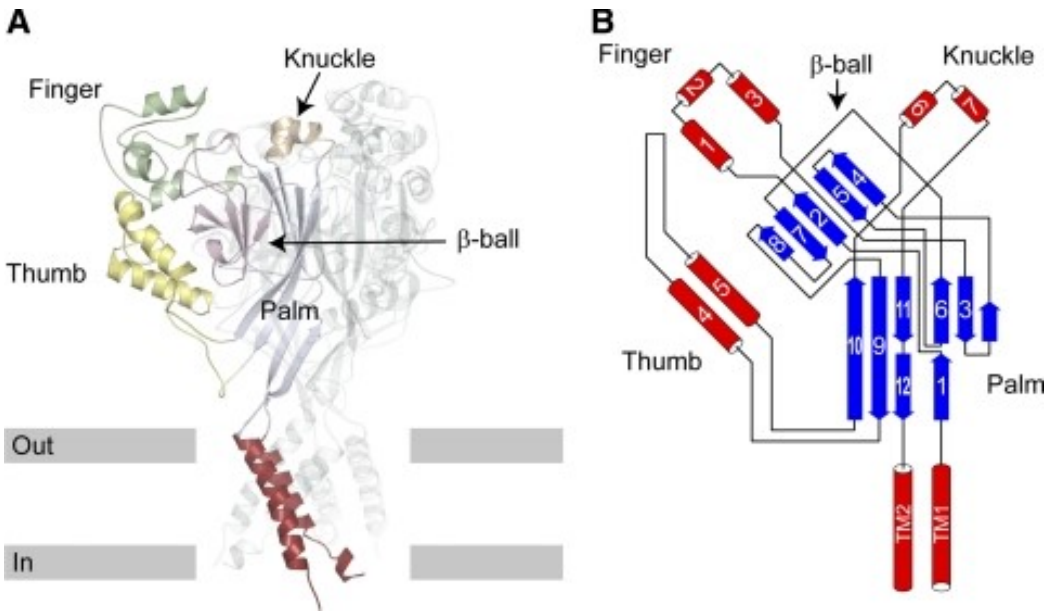

Fig. 3. Ribbon diagram (A) and topology diagram (B) of cASIC1. Like the other members of the DEG/ENaC superfamily, the three subunits of cASIC1 have two membrane-spanning α-helical regions, connected by a large extracellular loop and intracellular amino- and carboxyl-termini. Various domains in the extracellular loop are shown, including the palm and the β-ball, which show high sequence identity to ENaC. **A:** Only one subunit of the trimer is shown as a solid ribbon. The approximate position of the cell membrane is depicted in grey. **B:** α-Helices are represented by red cylinders and β-strands by blue arrows (Kashlan and Kleyman, 2011).

1.3. Pulmonary Edema

Pulmonary edema is defined as an accumulation of extravascular fluid in the lungs and may develop either as a result of elevated vascular pressure or an increase in lung vascular and epithelial permeability (Murray, 2011; Matthay, 2014). In general, the lung is capable of removing excess alveolar fluid (i.e. at birth or under pathological conditions leading to the development of pulmonary edema) by vectorial salt and water transport across the alveolar and distal airway epithelium (Matthay et al., 2002).

1.3.1. Distal pulmonary epithelium

The interface between lung parenchyma and the external environment is made up by the airways and alveoli, which are lined by a continuous epithelium (Matthay et al., 2002). An asymmetrical distribution of ion channels and other membrane proteins in the pulmonary epithelium enables these cells to vectorially transport Na^+ and Cl^- followed by osmotically driven water movement (Folkesson and Matthay, 2006; Eaton et al., 2009). The distal airway epithelium contains ciliated Clara cells and nonciliated cuboidal cells, whereas the alveolar epithelium is composed of thin, squamous type I cells and cuboidal type II cells (Fig. 4) (Matthay et al., 2002). Alveolar type I cells (AT1) and alveolar type II cells (AT2) are linked by tight junctions in order to sustain apical and basolateral cell polarity (Folkesson and Matthay, 2006). A thin basal lamina at the basolateral side separates the alveolar epithelium from the small interstitium and the pulmonary capillaries (Althaus et al., 2011).

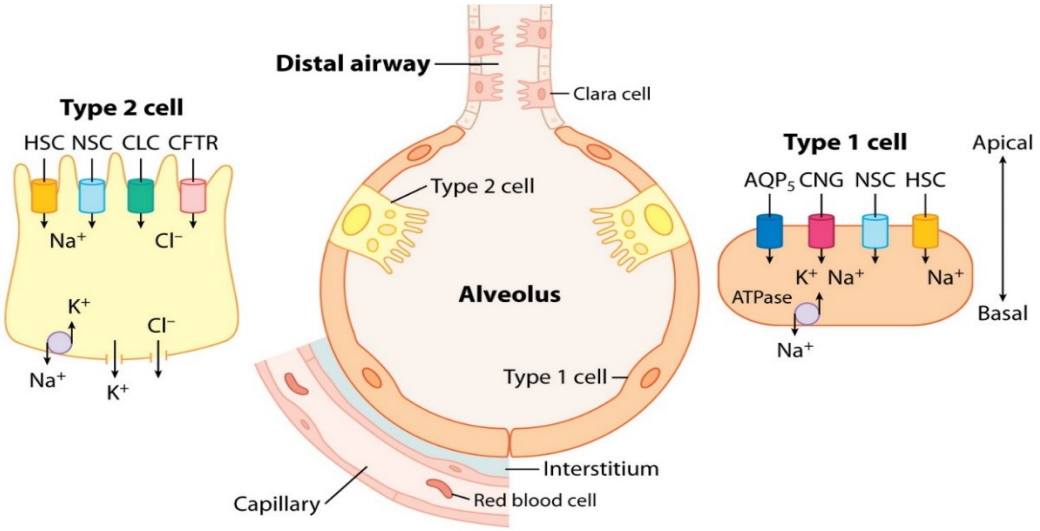

Fig. 4. Schematic diagram of an alveolus and part of the distal airways.
(*Left)* Alveolar type II cells (AT2) only make up 2-5% of the internal surface area of the lung and are responsible for secretion of pulmonary surfactant. AT2 cells express numerous ion channels, including two different types of ENaC: a highly Na^+-selective channel (HSC) and a cation-nonselective channel (NSC). Cl^- is transported via the cystic fibrosis transmembrane regulator (CFTR) and Cl^- channels (CLC). The basolateral membrane features the Na^+/K^+-ATPase. *(Right)* Alveolar type I cells (AT1) cover more than 95% of the internal surface area of the lung. Less is known about the AT1 cells and their contribution to alveolar fluid clearance. However, they also express a number of different ion channels, including HSC and NSC as well as cyclic nucleotide-gated channels (CNG). AT1 cells also feature a high concentration of aquaporin 5 (AQP_5) proteins on the apical membrane as well as Na^+/K^+-ATPase enzymes, which are located basolaterally (Eaton et al., 2009).

1.3.2. Alveolar fluid clearance (AFC)

For efficient gas exchange in the lungs a thin layer of liquid on the air-facing side of the alveolar epithelium is necessary (Eaton et al., 2009). The amount of this fluid on the airway surface is a result of liquid being forced from the capillaries into the alveolar airspaces due to blood pressure, and reabsorption by the alveolar epithelium, a process referred to as alveolar fluid clearance (AFC) (Eaton et al., 2009; Althaus et al., 2011).

The general paradigm is that ion transport across the alveolar epithelium drives AFC (Fig. 5) (Folkesson and Matthay, 2006; Berthiaume and Matthay, 2007; Eaton et al., 2009).

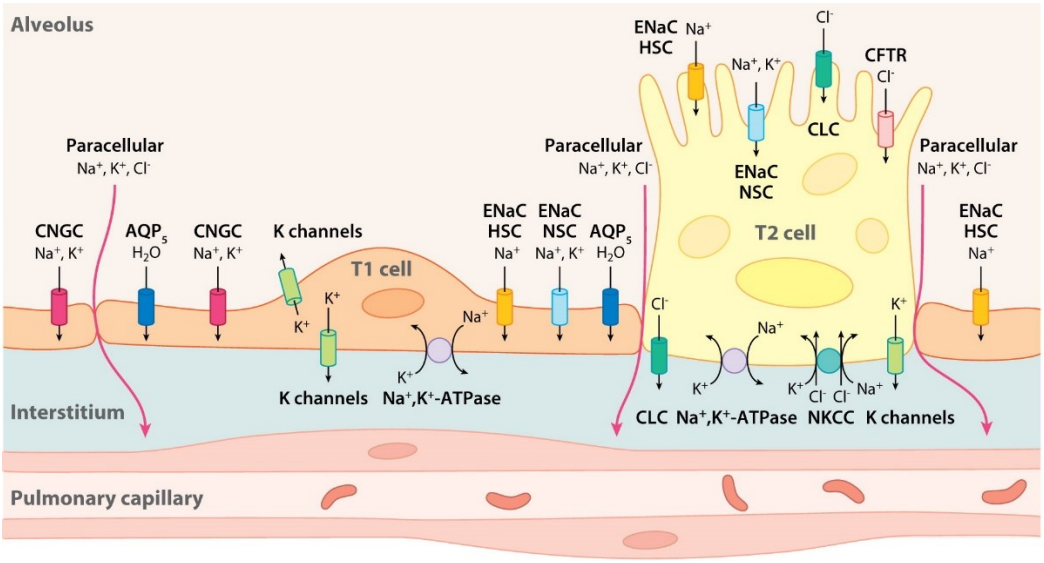

Fig. 5. Schematic diagram of alveolar epithelial transport. ENaC (HSC, NSC) is the main pathway for Na^+ absorption in both AT1 and AT2 cells. Subsequently, Na^+ is transported from these cells by Na^+/K^+-ATPase into the interstitial space. Cl^- movement through CFTR and Cl^- channels (CLC) conserves electroneutrality. An alternative, amiloride-insensitive pathway for Na^+ entry into the epithelium are cyclic nucleotide-gated channels (CNGC). AT2 cells also express Na-K-Cl cotransporters (NKCC) at the basolateral membrane. Paracellular movement of ions through tight junctions is possible, too. Net ion transport from the apical surface to the interstitium creates an osmotic gradient, which drives water movement via aquaporins (AQP) in the same direction (Eaton et al., 2009).

Amiloride-sensitive Na^+ absorption through ENaC plays a major role in alveolar fluid clearance (Matthay et al., 2002; Berthiaume and Matthay, 2007; Althaus et al., 2011). This role was highlighted by a study with α-ENaC deficient knockout mice, who die within two days of birth from failure to clear their lungs of liquid (Hummler et al., 1996).

1.3.3. Classification and therapy

A distinction between two main forms of pulmonary edema can be drawn (Murray, 2011). Each type occurs under different clinical conditions, requires separate therapy, and has a distinct prognosis (Murray, 2011).

1.3.3.1. Cardiogenic pulmonary edema

Cardiogenic pulmonary edema is a result of elevated pulmonary capillary pressure due to left ventricular heart failure (Murray, 2011).

Treatment of cardiogenic pulmonary edema depends on the underlying cause, but usually involves administration of intravenous diuretics and morphine along with oxygen therapy (Cleland et al., 2010). Some patients, who do not respond to conventional treatment, might require mechanical ventilation (Cleland et al., 2010).

1.3.3.2. Non-cardiogenic pulmonary edema

Non-cardiogenic pulmonary edema, clinically recognized as the acute respiratory distress syndrome (ARDS), is usually caused by an increase in lung vascular and epithelial permeability (Matthay, 2014). This condition results from injury to the lungs sufficient to prompt extravasation of fluid into the interstitial and alveolar spaces (Murray, 2011). Most patients with ARDS have impaired alveolar fluid clearance, a finding associated with prolonged respiratory failure and higher mortality (Ware and Matthay, 2001).

The only treatment option currently available for patients with non-cardiogenic pulmonary edema is mechanical ventilation (Johnson and Matthay, 2010).
To date no pharmacologic strategies have proven useful in reducing mortality (Johnson and Matthay, 2010). A number of phase III trials failed to show a significant benefit of administering exogenous surfactant, glucocorticoids, N-acetylcysteine and activated protein C (Johnson and Matthay, 2010). β-agonists showed promising results in early studies, but were discarded after larger scale trials yielded no desirable outcomes (Bassford et al., 2012).

1.4. AP301

AP301 (proprietary name: solnatide) is a fully synthetic peptide, mimicking the lectin-like domain (labelled TIP domain) of TNF-α (Hazemi et al., 2010; Mascher et al., 2012).

A nebulised formulation of AP301 is currently being evaluated in clinical trials for use in patients suffering from pulmonary edema. Meanwhile, a recent study investigating the effect of inhaled doses of AP301 on alveolar fluid clearance in acute lung injury (ALI) yielded promising results (Department of Anesthesia and Intensive Care Medicine, Medical University Vienna; ClinicalTrials.gov Identifier: NCT01627613). Of late, phase III clinical development strategy for AP301 in ARDS has been confirmed by the European Medicines Agency (EMA) (APEPTICO - Innovation in peptide drugs - Vienna, Austria, 2015).

Very recently, the Committee for Orphan Medicinal Products of the EMA has granted AP301 orphan drug designation for the orphan indication “treatment of primary graft dysfunction following lung transplantation“ (Fischer, 2015).

1.4.1. Development

Although TNF-α is a potent mediator of inflammation and has been linked with progression of ARDS (Lucas et al., 1997) among other pulmonary diseases, this cytokine is also capable of upregulating alveolar fluid clearance (Rezaiguia et al., 1997; Börjesson et al., 2000). The increase in amiloride-sensitive current across distal airway epithelia involves activation of Na^+ channels through binding of TNF-α via its lectin-like domain (Fukuda et al., 2001; Elia et al., 2003; Braun et al., 2005; Hazemi et al., 2010).

Based on these findings, a series of cyclic peptides that mimic the lectin-like domain of TNF-α were synthesised, one of which – TIP peptide 1 – was later termed AP301 (Hazemi et al., 2010).

The Na^+ channel responsible for this effect of TNF-α on alveolar fluid clearance was found to be ENaC (Shabbir et al., 2013; Tzotzos et al., 2013). Although the exact mechanism of action remains unclear, a recent study suggests cellular uptake and subsequent binding of the TIP domain to the carboxy-terminus of α-ENaC, resulting in preservation of channel expression (Czikora et al., 2014).

1.4.2. Structure

AP301 is a cyclic peptide, which is comprised of 17 amino acids [Cyclo(CGQRETPEGAEAKPWYC)] (Hazemi et al., 2010). Fig. 6 explains important structural features necessary for ENaC activation and highlights the similar structure of the TIP domain of human TNF-α and AP301.

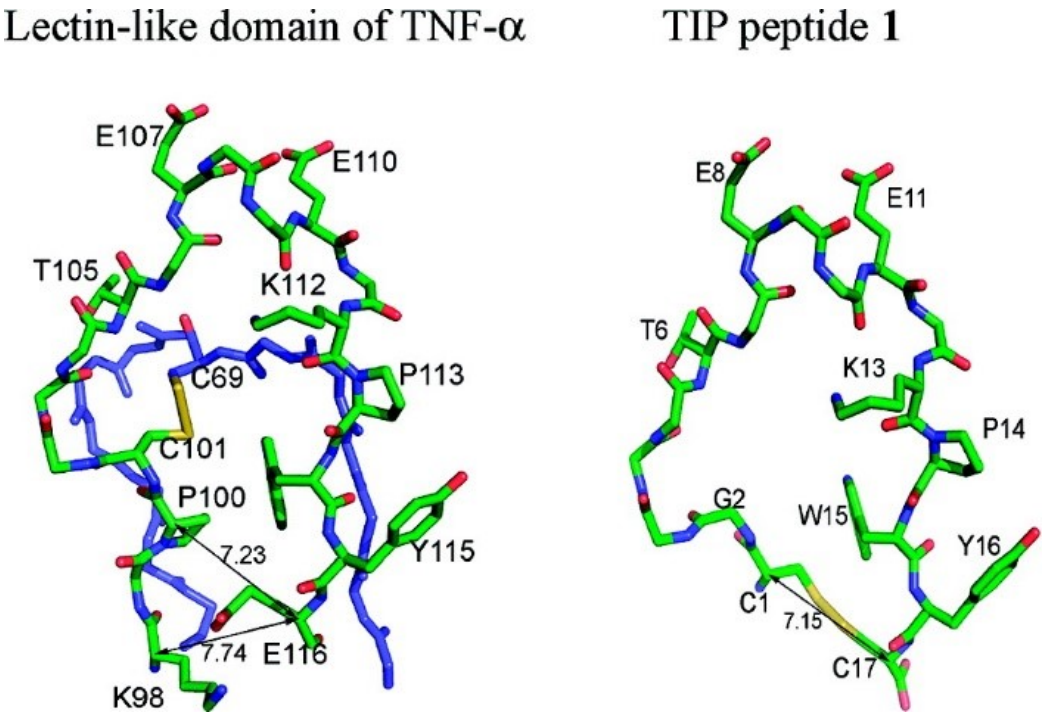

Fig. 6. The TIP or lectin-like domain of human TNF-α (C101-E116) according to structure PDB ID: 1A8M and a model for the TIP peptide 1 (later termed AP301) are shown. Amino acid residues essential for ENaC activation are T105, E107 and E110 in human TNF-α. Corresponding residues in AP301 are T6, E8 and E11. Other structural properties relevant for an ENaC-activating effect include a group of adjacent hydrophobic residues equivalent to P113, W114 and Y115 of human TNF-α and a positively charged N-terminal amino group or a negatively charged C-terminal carboxyl group or both of these. Numbers adjacent to lines with double arrowheads refer to Cα−Cα distances in Å. Disulfide bridges between cysteine residues are depicted in yellow (Hazemi et al., 2010).

1.4.3. Experimental Data

Various studies using the patch-clamp technique have been conducted to assess the effect of AP301 on Na^+ currents in cells expressing ENaC.

In A549 cells, a human lung adenocarcinoma cell line expressing ENaC endogenously, AP301 greatly enhanced amiloride-sensitive Na^+ current, eliciting an increase of about 20-fold in whole-cell recordings (Hazemi et al., 2010). A study utilising primary dog, rat and pig alveolar type II cells showed an increase in amiloride-sensitive Na^+ current of roughly 16-fold across species (Tzotzos et al., 2013).

In heterologous expression systems, namely CHO and HEK-293 cells transfected with hENaC subunits, AP301 addition provoked a 10-fold increase in ENaC-mediated Na^+ current (Shabbir et al., 2013). The same study also investigated the necessity of proteolytic activation and glycosylation of ENaC for the effect of AP301. RPMI-2650 cells, a human nasal epithelial cell line, endogenously express hENaC mainly in a near-silent conformation, requiring activation through proteolysis (Prulière-Escabasse et al., 2010). For a response to AP301, proteolytic cleavage of ENaC in RPMI-2650 cells is required, indicating that AP301 can only enhance currents in proteolytically processed channels (Shabbir et al., 2013). Similarly, glycosylation of ENaC's extracellular domain is a requirement for channel activation by AP301 (Shabbir et al., 2013).

2. Materials and methods

All chemicals, reagents and culture media were obtained from Sigma-Aldrich (Vienna, Austria) unless stated otherwise.

2.1. Cell Culture

2.1.1. Cell Lines

Three different cell lines were used:

1) A549 cells (ATCC no. CCL-185), a human lung adenocarcinoma cell line with alveolar type II cell morphology, were kindly supplied by W. Berger (Department of Medicine I, Institute of Cancer Research, Medical University of Vienna, Vienna, Austria) in the 80th passage.
2) RPMI-2650 cells (ATCC no. CCL-30) are derived from squamous cell carcinoma of the nasal septum and show epithelial morphology. This cell line was purchased from American Type Culture Collection (Manassas, VA).
3) HEK-293 cells (ATCC no. CRL-1573), a human embryonic kidney cell line, were also acquired from American Type Culture Collection (Manassas, VA).

Cell lines were used in passages 80-97 for A549 cells, passages 8-24 for RPMI-2650 cells and passages 3-25 for HEK-293 cells, respectively.

2.1.2. Thawing cells

Cells were stored in the vapour phase of liquid nitrogen for long-term preservation using cryovials. For seeding, cells were thawed in a water bath (37 °C) under light agitation. Before thawing was finished, the vials were cleaned with ethanol 70% on the outside and transferred into the tissue culture hood. To remove DMSO contained in freezing medium, the cell suspension was diluted with 8 ml growth medium (see Table 1) and spun down. After discarding the supernatant, cells were resuspended in growth medium and seeded in a tissue culture flask to be maintained in an incubator (37 °C and 5% CO_2).

2.1.3. Cultivation

All cell lines were cultivated in DMEM/F-12 [Dulbecco's modified Eagle medium/F12 nutrient mixture Ham + L-Glutamine (Gibco™ by Life Technologies, LifeTech Austria)], supplemented with 10% fetal bovine serum (FBS) and 1% penicillin-streptomycin. Cells were maintained either in T75 tissue culture flasks (ThermoScientific™ BioLite) for cultivation or in 100mm dishes (Thermo Scientific™ BioLite) for treatment and subsequent protein isolation.

Cell cultures were observed regularly for confluence and changes in morphology. At about 80% confluence (10^7 cells), cells were either split for further use or treated with AP301 (see 2.1.7. Cell treatment).

2.1.4. Splitting cells

Growth medium was aspirated and the cell layer was washed with phosphate buffered saline (PBS) without Ca^{2+}/Mg^{2+} (see Table 1) once to remove residual medium. Following aspiration of PBS, cells were detached from the flask with 0.05% trypsin/EDTA solution containing phenol red. To stop trypsin digestion after a few minutes of incubation, growth medium was added to the cell suspension. After resuspending the cell mass to allow even distribution, an appropriate amount of cell suspension was transferred into new tissue culture flasks or dishes for further cultivation.

2.1.5. Freezing cells

For cryopreservation, cells were detached with trypsin/EDTA and resuspended in DMEM/F-12. Following centrifugation at 500 g for 5 min and aspiration of the supernatant, cells were resuspended in growth medium. This cell suspension was diluted 1:1 with freezing medium (see Table 1) and transferred into cryovials, which were kept on ice for cooling. To avoid rapid cooling and killing of cells, cryovials were placed inside a passive freezer filled with isopropanol (rate of cooling approximately 1 °C/min) to be stored at -80 °C. A week later, one vial was thawed to check cell viability. Afterwards, remaining cryovials were moved to the vapour phase of a liquid nitrogen storage vessel for long-term preservation.

Growth medium	DMEM/F-12 supplemented with: 10% fetal bovine serum (FBS) 1% penicillin-streptomycin
Freezing medium	DMEM/F-12 supplemented with: 40% fetal bovine serum (FBS) 10% dimethyl sulfoxide (DMSO)
PBS without Ca^{2+}/Mg^{2+}	137 mM NaCl 2.7 mM KCl 10 mM Na_2HPO4 1.8 mM KH_2PO4 pH 7.4 (adjusted with HCl) (solution was autoclaved for use in cell culture)

Table 1 Cell culture media and reagents

2.1.6. Transfection

HEK-293 cells do not express ENaC subunits endogenously (Ruffieux-Daidie et al., 2008) and were therefore used as a heterologous expression system to study mutated hENaC proteins.

Transfection was performed 24 h after seeding of cells in tissue culture dishes. 50 µl K2® multiplier was added to each dish 2 h prior to transfection. 500 ng cDNA of each hENaC subunit and 20 µl K2® transfection reagent were diluted in DMEM/F-12 without FBS and carefully resuspended. This mixture was incubated at room temperature for 20 min to allow formation of lipoplexes. Subsequently, this solution was applied to cell culture dishes pre-incubated with K2® multiplier. 24 h after transfection, the medium was replaced with fresh growth medium to avoid toxic effects of the transfection reagent. Maximum expression levels (about 80% transfection efficiency) were seen 48 to 72 h post transfection. Transfection was monitored using a fluorescence microscope at 475 nm wavelength.

Enhanced green fluorescent protein (GFP)-tagged cDNAs encoding α-, β- and γ-hENaC were a kind gift from Dr. Deborah L. Baines (St. George's, University of London, London, UK). cDNA encoding δ-hENaC was a kind gift from Dr. Mike Althaus (Justus-Liebig University, Giessen, Germany).

Site-directed mutagenesis of α-hENaC cDNA to generate partly or completely unglycosylated α-hENaC proteins was carried out by Minela Hasanovic, B.Sc. and has been described previously (Hasanovic, 2013).

2.1.7. Cell treatment

After reaching confluence half of the growth medium was substituted with either DMEM/F-12 without FBS (for control) or DMEM/F-12 without FBS containing AP301 to reach a final concentration of 200 nM, a concentration at which a maximal effect was observed in electrophysiological experiments (Hazemi et al., 2010). Cell treatment was carried out in a time-dependent manner (5, 10, 30, 60 min, respectively).

The peptide AP301 was synthesised by solid-phase peptide synthesis according to the fluorenylmethyloxycarbonyl/*t*-butyl protection strategy on 2-chlorotritylchloride resin by Senn Chemicals AG, Dielsdorf, Switzerland (Tzotzos et al., 2013). Details of the synthesis have been described (Hazemi et al., 2010). The purity of the peptide was 96.3%. m/z (ESI) 1924.2 (M^++1); theoretical average molecular mass 1923.1. (Tzotzos et al., 2013)

2.2. Protein isolation and quantification

2.2.1. Cell lysis

Following treatment, cells were washed twice with ice-cold PBS before extracting buffer (150 mM sodium acetate, 0.9% NaCl, 0.1% Triton X-100, pH 5.5) was applied. After scraping cells off the dishes, the resulting cell suspension was collected in vials and lysed using ultrasonication (3 x 10 s). Following incubation on ice for 30 min, cell debris was removed by centrifugation at 13.000 RPM/4 °C for 10 min. The supernatant containing whole-cell proteins was stored at -20 °C for further use.

2.2.2. Bradford protein assay

Bradford protein assay was performed to determine the total protein concentration of cell lysates. 5 µl whole-cell protein of each sample and bovine serum albumin (BSA) protein standards (concentrations ranging from 0.125 µg/µl to 2.0 µg/µl) were pipetted into a 96-well microplate (Thermo Scientific™) to be analysed in triplicate. 250 µl Quick Start™ Bradford 1x Dye Reagent (Bio-Rad Laboratories) was added to each well. After incubation at room temperature for 10 min, absorption at 595nm was measured using the Infinite® 200Pro multimode microplate reader (Tecan Austria). Protein concentrations of samples were determined by fitting a standard curve to the BSA protein standard absorption values.

2.3. Western blotting

2.3.1. SDS-PAGE

Whole-cell proteins were denatured by mixing with 4X sample buffer (see Table 2) and heated to 95 °C for 5 min. Equal amounts of protein were separated under reducing conditions by 7.5% sodium dodecyl sulfate-polyacrylamide gel electrophoresis (SDS-PAGE). A colour-coded prestained protein marker ranging from 10-175 kDa (Prism Protein Ladder ab115832, abcam®) was also applied to the gel.

Running gel	
ddH_2O	9.7 ml
30% acrylamide/bis	5 ml
Tris-HCl 1.5M (pH 8.8)	5 ml
SDS 10%	0.2 ml
Ammonium persulfate 10%	0.1 ml
TEMED	10 µl
Stacking gel	
ddH_2O	7.5 ml
30% acrylamide/bis	1.7 ml
Tris-HCl 0.5M (pH 6.8)	3.2 ml
SDS 10%	125 µl
Ammonium persulfate 10%	125 µl
TEMED	12.5 µl
10x Running buffer	
Tris base	30.3 g
Glycine	144.2 g
SDS	10 g
ddH_2O	ad 1000 ml
4x Sample buffer	
Glycerol	40%
Tris-HCl (pH 6.8)	240 mM
SDS	8%
Bromophenol blue	0.04%
β-Mercaptoethanol	5%
10x Tris-buffered saline (TBS)	
Tris base	24.2 g
NaCl	80.0 g
ddH_2O	ad 1000 ml

Table 2 Reagents used for Western blotting

2.3.2. Blotting

Following separation, proteins were transferred onto a polyvinylidene difluoride membrane (UltraCruz™ PVDF membrane 0.45µm sc-3723, Santa Cruz Biotechnology, Texas, USA) by semi-dry blotting (Trans-Blot® Turbo™ TransferSystem, Bio-Rad Laboratories, Vienna, Austria) at 25 V for 30 min.

2.3.3. Detection

For blocking of unspecific binding sites, membranes were incubated with 3% BSA in PBS containing 0.04% sodium azide at 4 °C overnight.

In order to detect bound hENaC proteins, membranes were incubated with primary antibody solutions (see Table 3) overnight at 4 °C. Subsequently, membranes were washed three times with 1x TBS-T (TBS with 0.1% Tween 20) and corresponding horseradish peroxidase-conjugated secondary antibodies (see Table 3) were applied. After incubation for 60-90 min at room temperature and washing four times with TBS-T solution, enhanced chemiluminescence (ECL) substrate (Amersham ECL Plus Western Blotting Detection Reagent, GE Healthcare, Vienna, Austria) was distributed evenly on the membranes. Following incubation for 2 min, membranes were exposed to X-ray films (Amersham Hyperfilm ECL, GE Healthcare, Vienna, Austria).

Target	**Source**	**Dilution**	**Santa Cruz Cat. #**
α-ENaC (NH_2-terminal)	goat	1 : 500	sc-22239
δ-ENaC	rabbit	1 : 500	sc-21015
β-Actin	mouse	1 : 200	sc-81178
anti-mouse IgG	rabbit	1 : 5000	sc-358914
anti-rabbit IgG	donkey	1 : 5000	sc-2313
anti-goat IgG	donkey	1 : 5000	sc-2020

Table 3: Antibodies used for Western blotting. All antibodies were acquired from Santa Cruz Biotechnology.

2.3.4. Quantification and statistical analysis

Exposed films were scanned and densitometric quantification of proteins bands was performed using ImageJ (NIH, Maryland, USA). Results are means ± SEM from the number of experiments (n) indicated in the corresponding figures. Unpaired t-test was performed using GraphPad Software (version 3.02, GraphPad Software, San Diego, CA) to assess statistical significance. Statistical significance was set at $p<0.05$. Origin 7 (Microcal Software) was used to calculate means and SEM, and to create column charts.

3. Results

Previous studies have assessed that the lectin-like domain (TIP domain) of TNF-α is capable of increasing amiloride-sensitive currents across alveolar epithelial cells (Fukuda et al., 2001; Elia et al., 2003). The channel responsible for mediation of this effect was found to be ENaC (Shabbir et al., 2013; Tzotzos et al., 2013).

AP301, a cyclic peptide which mimics this TIP domain, has been shown to activate ENaC in non-human primary alveolar type II cells and a variety of cell lines (Hazemi et al., 2010; Shabbir et al., 2013; Tzotzos et al., 2013; Czikora et al., 2014). It was established that this effect is in part mediated by increasing channel open probability (P_O) (Shabbir et al., 2013). However, an additional impact of AP301 on protein expression of ENaC could not be excluded (Shabbir et al., 2013).

A recent study showed that AP301 is capable of increasing α-ENaC expression in H441 cells (Czikora et al., 2014). The authors concluded that this effect is probably a result of AP301 binding to sugar moieties in the extracellular domain of ENaC, subsequent cellular uptake and finally binding to the C-terminal domain of the α subunit, thereby preserving α-ENaC expression (Czikora et al., 2014).

In this study this hypothesis was tested in two cell lines expressing ENaC endogenously, namely A549 and RPMI-2650. Along with α-ENaC, the δ subunit seems to act as the pore-forming element (Waldmann et al., 1995). It was previously established that α- or δ-hENaC, co-expressed with βγ subunits, is required for a current-enhancing effect of AP301 (Shabbir et al., 2013). Therefore, expression levels of these two pore-forming subunits were analysed through Western blotting.

The relevance of N-glycosylation of α-hENaC for the effect of AP301 was investigated in HEK-293 cells expressing partly or completely unglycosylated mutants of α-hENaC.

All cell cultures were treated with 200 nM AP301, based on previous results by Hazemi et al. indicating a maximal current-enhancing effect with 120 nM AP301 (Hazemi et al., 2010). Treatment was carried out in a time-dependent manner to establish the duration of a possible increase in ENaC expression.

3.1. Effect on α/δ-ENaC expression in A549 cells

AP301 has been shown to activate ENaC *in vitro* in A549 cells (Hazemi et al., 2010). Whole-cell recordings in patch-clamp experiments demonstrated a 20-fold increase in amiloride-sensitive Na^+ current in this cell line (Hazemi et al., 2010), which expresses all four ENaC subunits endogenously (Ji et al., 2006). A549 cells are a widely used cell line in ENaC research, noted for their overexpression of ENaC channels (Lazrak et al., 2000).

In this study A549 cells were treated with 200 nM AP301 for 5, 10, 30 and 60 min, respectively. Fig. 7 shows α-hENaC bands detected in Western blotting. α-ENaC is expressed in various isoforms in lung epithelial cells (Xu and Chu, 2007). The main isoforms are α_1 (~76 kDa) and α_2 (~85 kDa) (Thomas et al., 1998; Xu and Chu, 2007), which are clearly visible. Another band at 66 kDa is probably produced by proteolytic cleavage of α-ENaC (Garcia-Caballero et al., 2008). Untransfected HEK-293 cell lysate was also applied to test for unspecific antibody binding. HEK-293 cells do not express ENaC endogenously, but are known to contain proteins which give cross-reactions with α-ENaC antibodies (Ruffieux-Daidie et al., 2008). Previously detected expression of ASIC1a in HEK-293 cells might explain this observation (Gunthorpe et al., 2001). Due to the close relation of these two protein families, a cross-reaction seems likely.

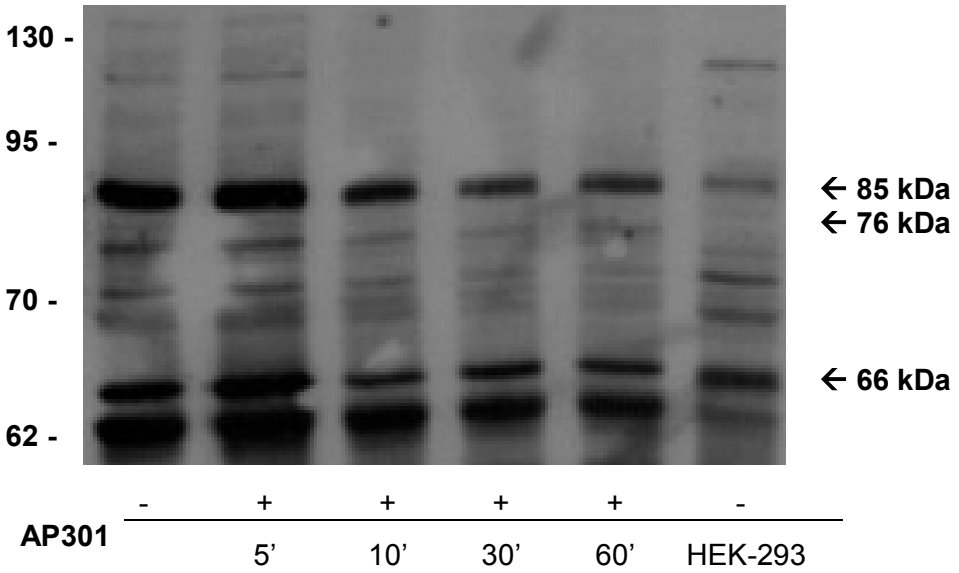

Fig. 7. Effect of 200 nM AP301 on expression of α-hENaC in A549 cells. Cell cultures were treated in a time-dependent manner. Time intervals of treatment (in min) are indicated at the bottom of the figure. Untransfected HEK-293 cell lysate was used as a control to check for unspecific binding of the antibodies. Approximate molecular weight (in kDa) on the image is depicted on the left. Important α-hENaC bands are labelled with arrows on the right-hand side.

Expression levels of α-hENaC (α_2 isoform at ~85 kDa) in A549 cell lysates treated with 200 nM AP301 from three independent biological replicates were quantified. Fig. 8 shows a transient increase in α-hENaC expression induced by AP301 of roughly 20% (1.18±0.09 fold, n = 3) compared to control, with a maximal effect after 5 min and steady decline afterwards. Expression levels return to baseline after 60 min. It has to be pointed out that statistical significance when comparing control and treated samples was only achieved in one case (10 min treatment).

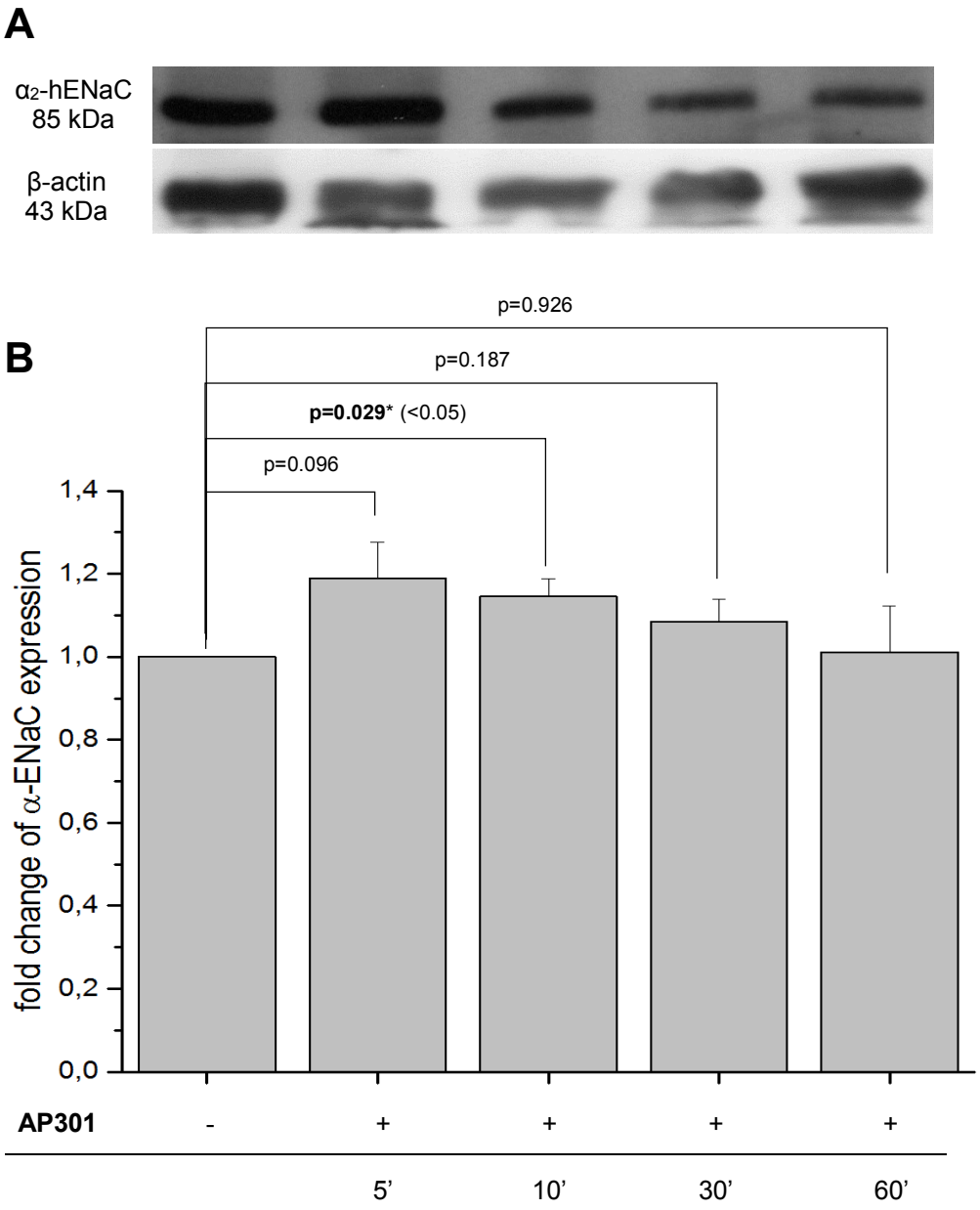

Fig. 8. Increase in expression levels of α-hENaC (α_2 isoform) in A549 cells treated with 200 nM AP301. β-actin was used as loading control. **A:** One representative image of protein bands is shown. **B:** A transient increase in α-hENaC expression is observed. Time intervals of treatment (in min) are indicated at the bottom of the figure. Results are shown as mean values ± SEM. p-values as determined by unpaired t-test are given. Statistical significance was set at $p<0.05$. *$p<0.05$ (n=3)

The same samples were incubated with δ-hENaC antibodies and detected with appropriate secondary antibodies. Resulting bands are shown in Fig. 9. Like the α subunit, δ-hENaC is expressed in numerous isoforms in lung epithelial cells (Ji et al., 2012), with δ_1 (~100 kDa) and δ_2 (~85 kDa) being the predominant ones (Ji et al., 2006, 2012; Zhao et al., 2012). A C-terminal fragment generated by proteolytic cleavage of δ-hENaC is detectable at 65 kDa (Haerteis et al., 2009). Cross-reactions of δ-hENaC antibodies with proteins (probably ASIC1a) of HEK-293 cells, as described for α-hENaC, seemed to occur here as well.

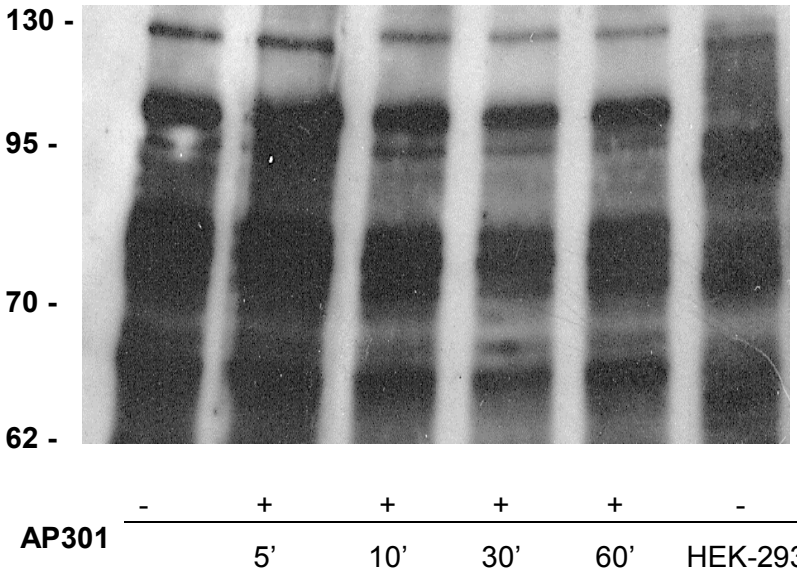

Fig. 9. Effect of 200 nM AP301 on expression of δ-hENaC in A549 cells. Cell cultures were treated in a time-dependent manner. Time intervals of treatment (in min) are indicated at the bottom of the figure. Untransfected HEK-293 cell lysate was used as a control to check for unspecific binding of the antibodies. Approximate molecular weight (in kDa) on the image is depicted on the left. Important δ-hENaC bands are labelled with arrows on the right-hand side.

Expression levels of δ-hENaC (δ_1 isoform at ~100 kDa) in A549 cell lysates treated with 200 nM AP301 from four independent biological replicates were quantified. A transient increase in δ-hENaC expression induced by AP301 is shown in Fig. 10, with a maximal effect after 10 min and steady decline afterwards. As with α-hENaC, expression is increased for about 20% (1.19±0.08 fold, n = 4). Expression levels return to baseline after 30 to 60 min. Unfortunately, statistical significance when comparing control and treated samples was not achieved in these experiments.

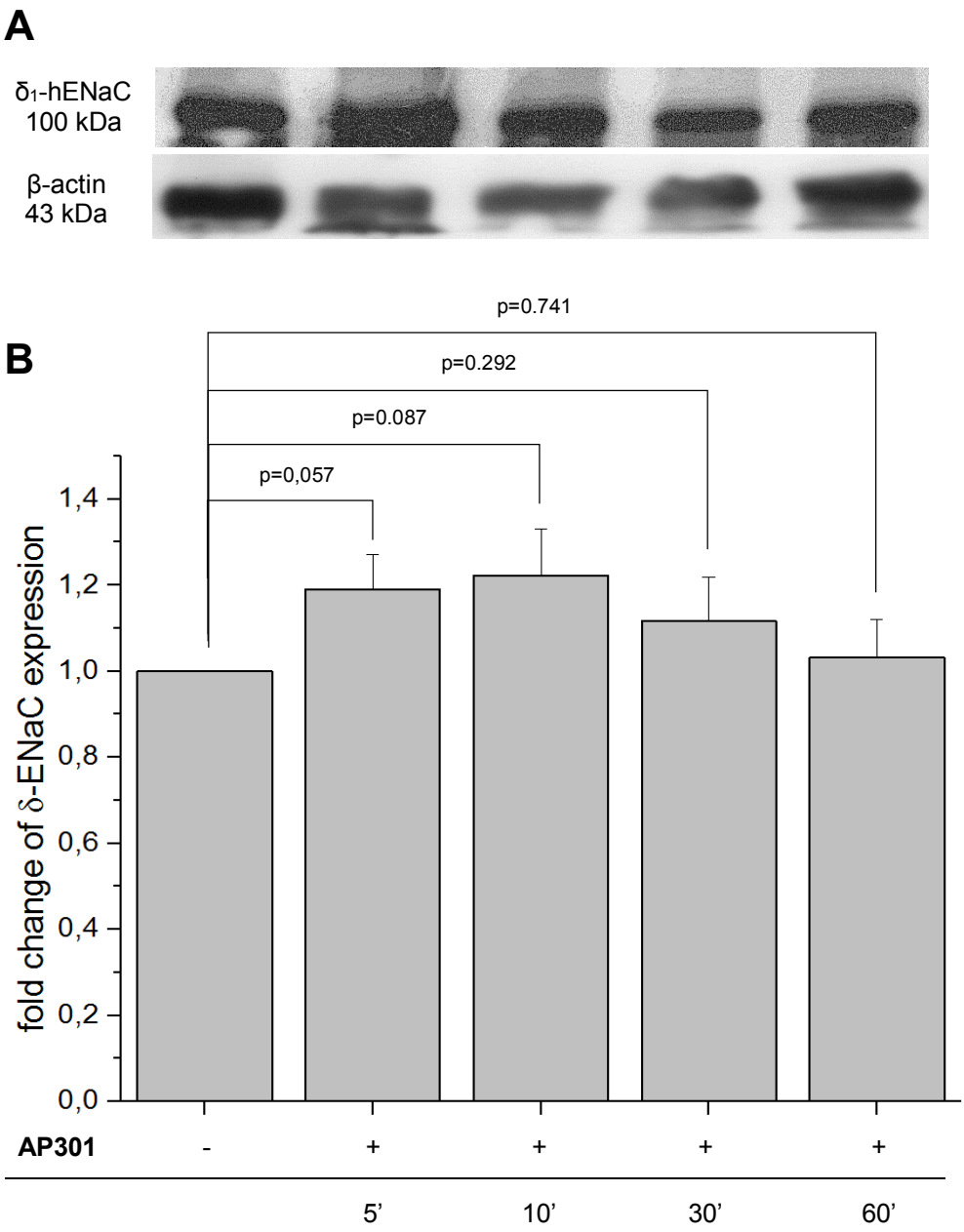

Fig. 10. Increase in expression levels of δ-hENaC (δ_1 isoform) in A549 cells treated with 200 nM AP301. β-actin was used as loading control. **A:** One representative image of protein bands is shown. **B:** A transient increase in δ-hENaC expression is observed. Time intervals of treatment (in min) are indicated at the bottom of the figure. Results are shown as mean values ± SEM. p-values as determined by unpaired t-test are given. Statistical significance was set at $p<0.05$. (n=4)

In summary, AP301 seems to be able to transiently increase expression of α- and δ-hENaC in A549 cells, when used at a concentration of 200 nM. However, statistical significance for these experiments was poor, so these results should be considered with caution.

3.2. Effect on α-/δ-ENaC expression in RPMI-2650 cells

The same current-enhancing effect of AP301 on ENaC as described above for A549 cells could also be observed in a patch-clamp study using RPMI-2650 cells (Shabbir et al., 2013), a nasal epithelial cell line derived from squamous cell carcinoma. Human nasal epithelial cells also express all four ENaC subunits endogenously (Bangel et al., 2008; Bangel-Ruland et al., 2010), though mainly in a near-silent conformation and therefore require proteolytic activation (Prulière-Escabasse et al., 2010). Proteolysis was also shown to be a prerequisite for ENaC activation by AP301 in RPMI-2650 cells (Fig. 11) (Shabbir et al., 2013).

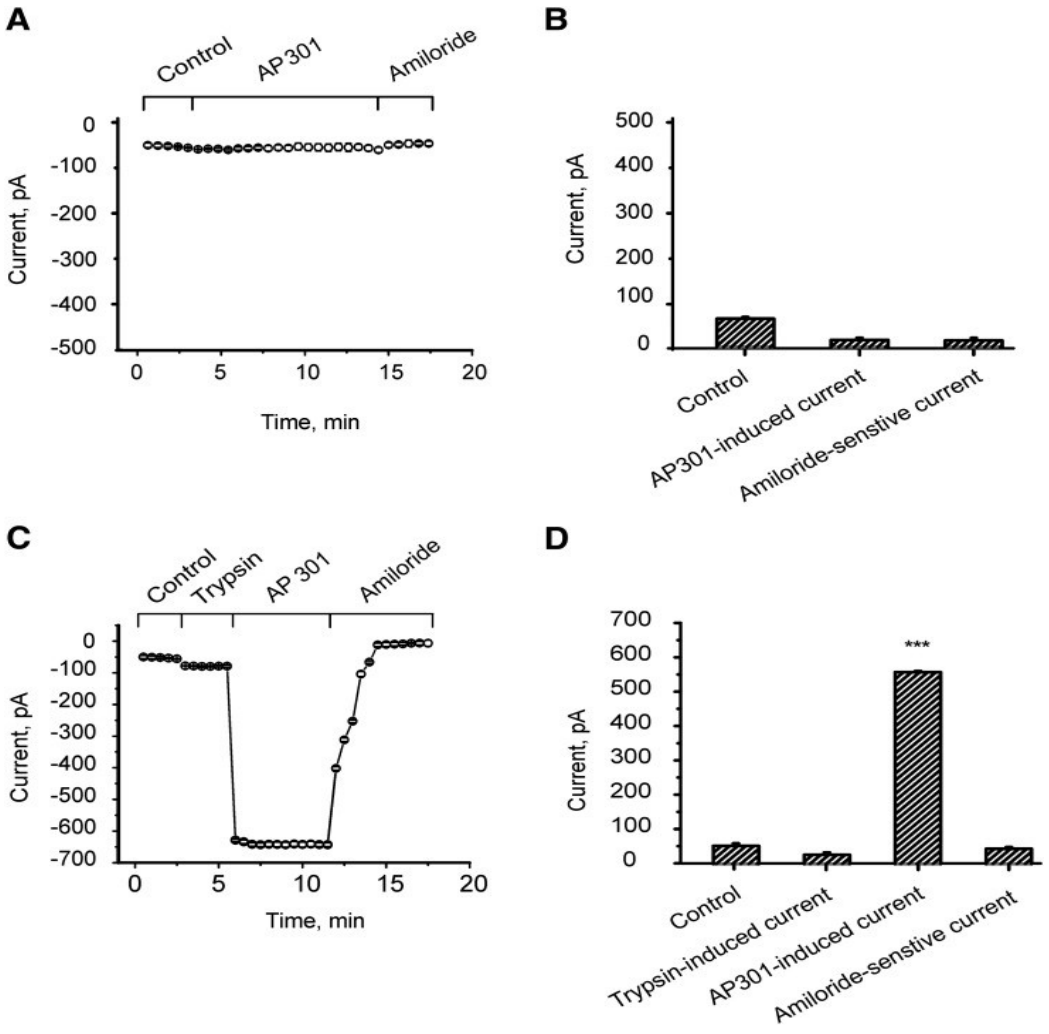

Fig. 11. Effect of AP301 on amiloride-sensitive sodium current in RPMI-2650 cells. Whole-cell recordings of cells at -100 mV holding potential are shown. **A and B:** AP301 did not induce inward sodium current from hENaC endogenously expressed in RPMI-2650 cells. **C and D:** After treatment with trypsin and subsequent application of AP301, proteolytically cleaved hENaC proteins could be activated by AP301 (Shabbir et al., 2013).

This study therefore analysed if homologous protein expression of α- and δ-hENaC could be increased with AP301 treatment in RPMI-2650 cells.

Thus, RPMI-2650 cells were treated with 200 nM AP301 for 5, 10, 30 and 60 min, respectively. Fig. 12 shows α-hENaC bands detected in Western blotting. Very little data exists on the expression of α-ENaC in nasal epithelial cells. One research group found two bands at roughly 66 and 55 kDa in nasal polyp tissue (Bangel et al., 2008), whereas others detected α-hENaC at 95 kDa in similar tissues (Jiang et al., 2015). In contrast, this study found only one α-hENaC band at 85 kDa, corresponding to the α_2 isoform found in A549 cells. The presence of only one protein band could probably be explained by the fact, that RPMI-2650 cells express ENaC mainly in a conformation not processed by proteolytic enzymes (Prulière-Escabasse et al., 2010) and therefore have very little amount of ENaC fragments. These results further indicate that RPMI-2650 cells possibly only express the α_2 isoform of hENaC.

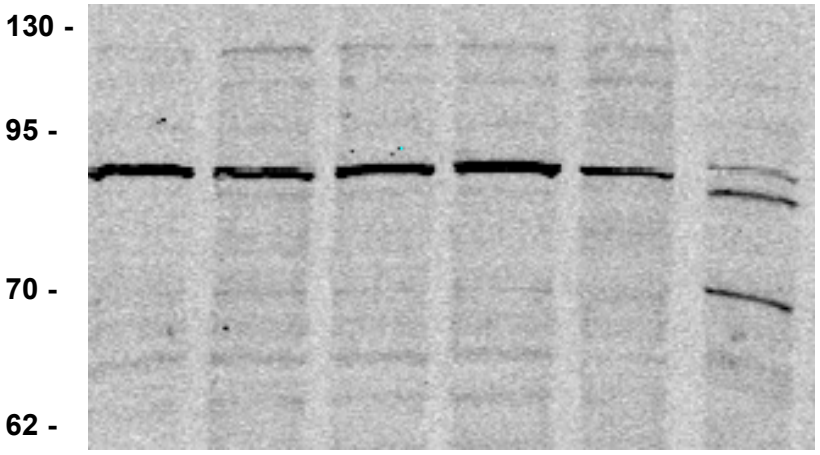

Fig. 12. Effect of 200 nM AP301 on expression of α-hENaC in RPMI-2650 cells. Cell cultures were treated in a time-dependent manner. Time intervals of treatment (in min) are indicated at the bottom of the figure. Untransfected HEK-293 cell lysate was used as a control to check for unspecific binding of the antibodies. Approximate molecular weight (in kDa) on the image is depicted on the left. Important α-hENaC bands are labelled with arrows on the right-hand side.

Quantified expression levels of α-hENaC (α_2 isoform at ~85 kDa) in RPMI-2650 cell lysates treated with 200 nM AP301 from two independent biological replicates are given in Fig. 13. A transient increase in α-hENaC expression induced by AP301 of roughly 12% (1.12±0.14 fold, n = 2) compared to control can be observed. This effect was only appreciable after 5 min and quickly diminished with

longer treatment intervals. However, results were quite inhomogeneous and did not achieve statistical significance.

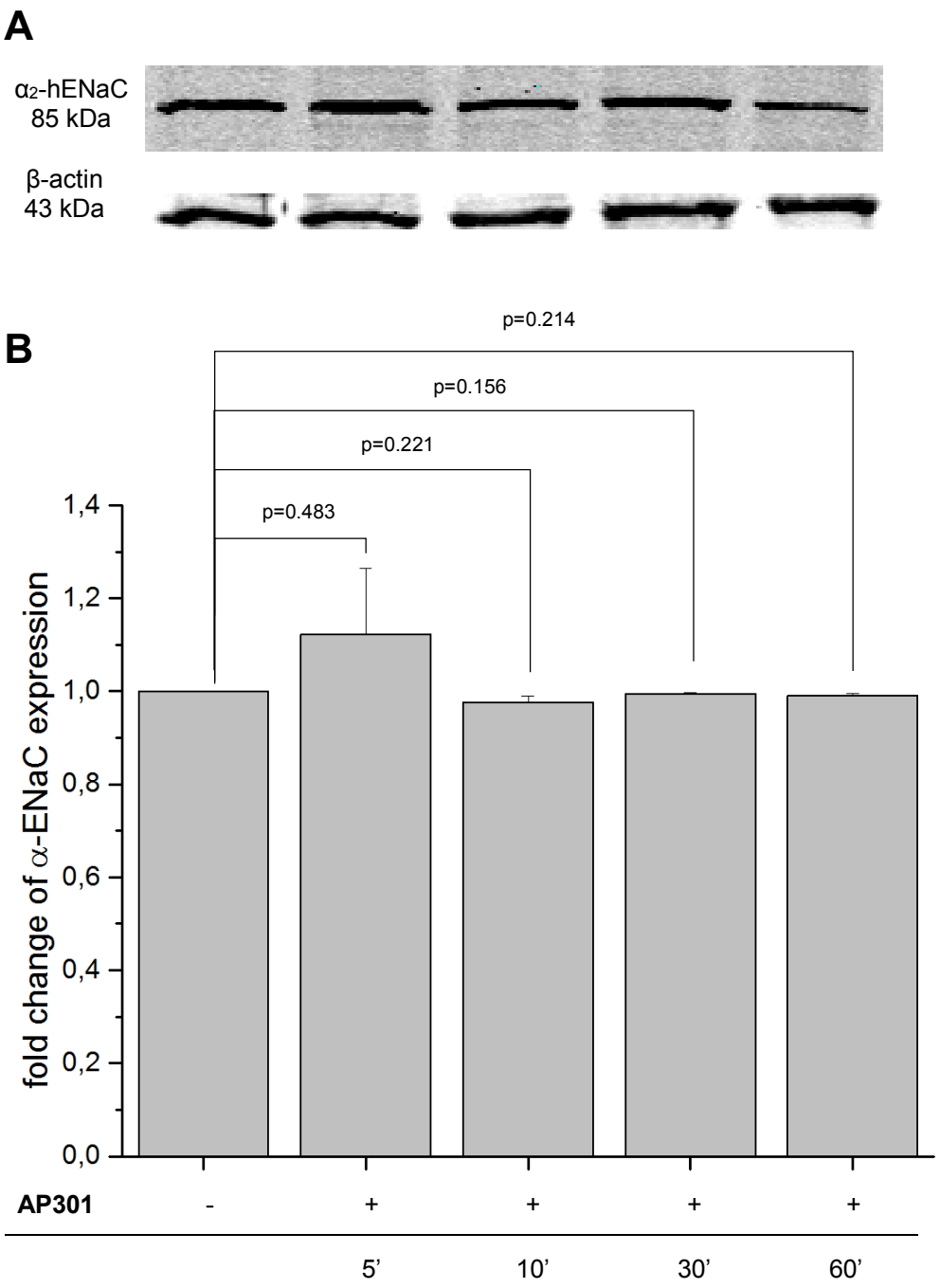

Fig. 13. Increase in expression levels of α-hENaC (α_2 isoform) in RPMI-2650 cells treated with 200 nM AP301. β-actin was used as loading control. **A:** One representative image of protein bands is shown. **B:** A transient increase in α-hENaC expression is observed. Time intervals of treatment (in min) are indicated at the bottom of the figure. Results are shown as mean values ± SEM. p-values as determined by unpaired t-test are given. Statistical significance was set at $p<0.05$. (n=2)

Bangel-Ruland et al. demonstrated the expression of an isoform of δ-ENaC in human nasal epithelial cells with a molecular weight of roughly 100 kDa (Bangel-Ruland et al., 2010). This δ isoform, which most likely corresponds to the δ_1 subunit found in A549 cells, was also detected in this study (Fig. 14). Another protein band at 85 kDa was appreciable, which could be attributed to the presence of δ_2-hENaC in RPMI-2650 cells.

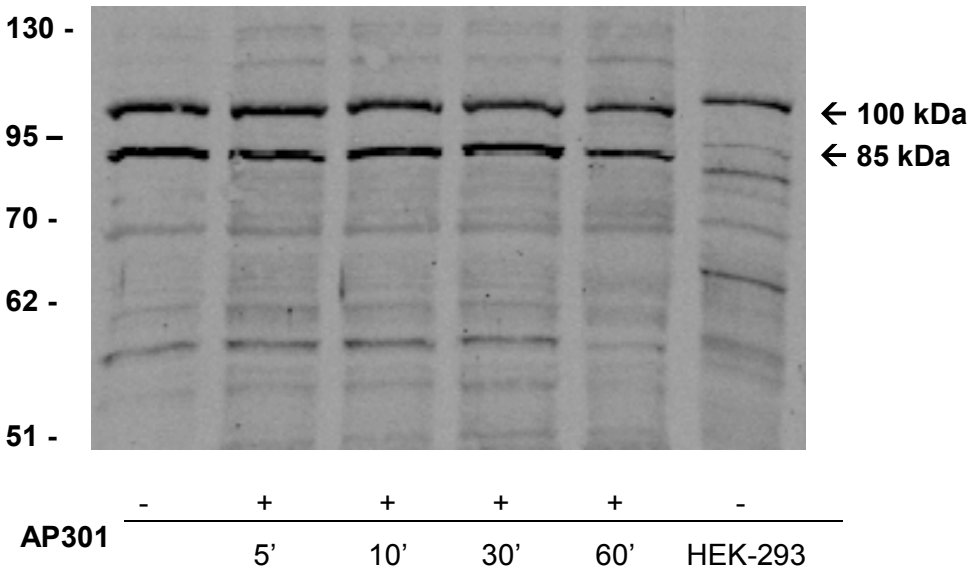

Fig. 14. Effect of 200 nM AP301 on expression of δ-hENaC in RPMI-2650 cells. Cell cultures were treated in a time-dependent manner. Time intervals of treatment (in min) are indicated at the bottom of the figure. Untransfected HEK-293 cell lysate was used as a control to check for unspecific binding of the antibodies. Approximate molecular weight (in kDa) on the image is depicted on the left. Important δ-hENaC bands are labelled with arrows on the right-hand side.

Quantification of expression levels of δ-hENaC (δ_1 isoform at ~100 kDa) in RPMI-2650 cell lysates treated with 200 nM AP301 from two independent biological replicates is given in Fig. 15. Almost no increase in expression could be observed in these experiments (1.02±0.02 fold, n = 2). Again, results did not achieve statistical significance.

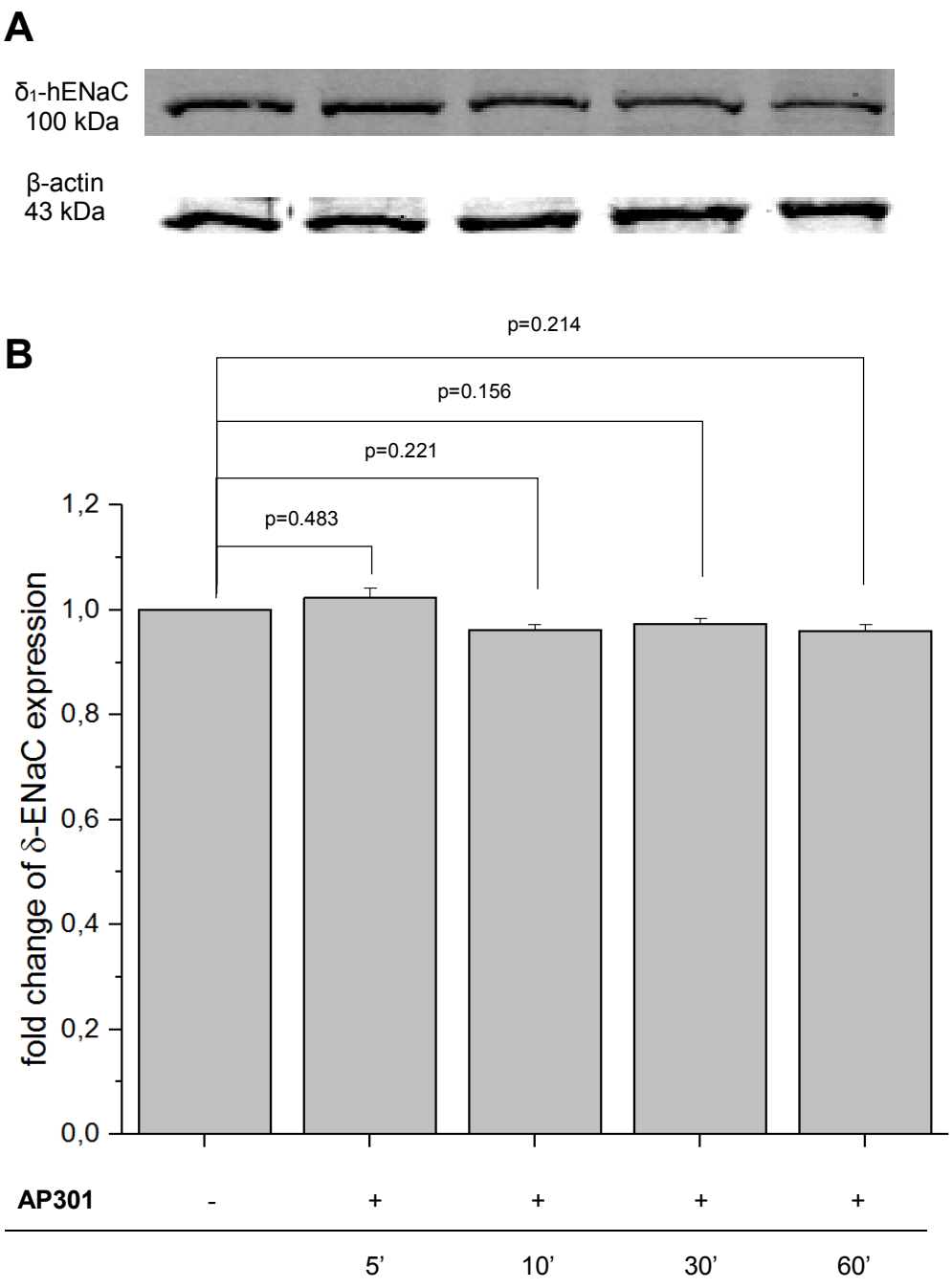

Fig. 15. Expression levels of δ-hENaC (δ_1 isoform) in RPMI-2650 cells treated with 200 nM AP301. β-actin was used as loading control. **A:** One representative image of protein bands is shown. **B:** No increase of δ-hENaC expression could be observed. Time intervals of treatment (in min) are indicated at the bottom of the figure. Results are shown as mean values ± SEM. p-values as determined by unpaired t-test are given. Statistical significance was set at $p<0.05$. (n=2)

In summary, these results indicate that AP301 might be able to transiently increase expression of α-hENaC in RPMI-2650 cells, when applied at a concentration of 200 nM. Almost no increase was observed for δ-hENaC. This data is however highly speculative, due to the low number of experiments (n=2).

3.3. Effect on unglycosylated α-hENaC mutants in HEK-293 cells

ENaC subunits have numerous sites for N-linked glycosylation in their extracellular domain (Prince and Welsh, 1998). The amount of glycosylated residues varies between subunits (Valentijn et al., 1998).

Previously, it was demonstrated in a molecular docking and dynamics simulation study that the lectin-like domain of TNF-α represents a partial binding motif for the disaccharide N,N'-diacetylchitobiose (Dulebo et al., 2012).

Patch-clamp experiments have highlighted the importance of glycosylation in the extracellular domain for the current-enhancing effect of AP301 on ENaC (Shabbir et al., 2013). Deglycosylation of A549 cells and HEK-293 cells, transfected with hENaC, using peptide-N4-(N-acetyl-β-D-glucosaminyl)asparagine amidase (PNGase F, glycopeptide N-glycosidase) abolished inward current activation by AP301 (Shabbir et al., 2013).

Recently published data by Czikora et al. implicate glycosylated residues in the extracellular region of ENaC with binding and subsequent cellular uptake of AP301 (Czikora et al., 2014).

This study therefore analysed if AP301 is capable of increasing expression of α-hENaC in HEK-293 cells transfected with either wild type (WT) or mutated α-hENaC cDNA lacking one or more N-glycosylation sites. Asparagine residues in these mutated proteins were replaced with glutamine to preserve biophysical properties, while inhibiting N-glycosylation. β- and γ-hENaC were co-expressed together with these α subunits. Of the five N-glycosylation sites in α-hENaC's extracellular domain, either the first (N232Q), the last (N511Q) or all (N232,293,312,397,511Q) were replaced with glutamine.

Based on the effect on ENaC expression observed in A549 cells, which was maximal after 5 min, cell cultures were treated with 200 nM AP301 for this duration.

Fig. 16 shows the main band, which was detected with α-hENaC antibodies in Western blotting experiments, at roughly 110 kDa. This protein band corresponds to an unidentified isoform. Another band at 85 kDa was discernible, which is probably α_2-hENaC as observed in the two other cell lines (not shown).

It is important to note that the lack of N-glycans in the mutated α subunits causes a shift in molecular weight (not shown), as described previously by other research groups (Canessa et al., 1994a; Snyder et al., 1994)..

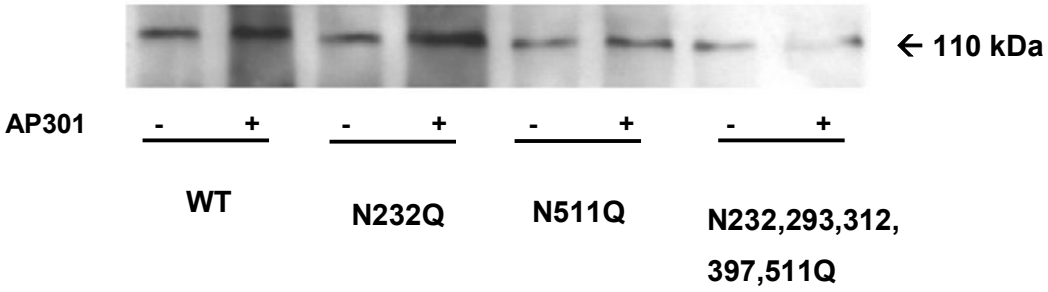

Fig. 16. Effect of 200 nM AP301 on expression of WT or α-hENaC mutants in HEK-293 cells. Cells expressed either WT or mutated α-hENaC lacking one or all N-glycosylation sites in the extracellular domain. α subunits were co-expressed together with β- and γ-hENaC. Cultures were either treated with growth medium (control) or AP301 for 5 min, as indicated on the bottom of the figure. Approximate molecular weight of the observed band is depicted on the right.

Expression levels of α-hENaC (~110 kDa) in HEK-293 cell lysates transfected with α-hENaC WT or N-glycosylation mutants from four to seven independent biological replicates were quantified. Fig. 17 shows a significant increase in α-hENaC WT expression induced by AP301 of roughly 50% (1.50±0.06 fold, $n = 7$, $p<0.01$) compared to control. A weaker but still significant increase is appreciable in the N232Q mutant (1.45±0.15 fold, $n = 4$, $p<0.01$).

No effect was visible in α-hENaC lacking N511 or all N-glycosylation sites (N232,293,312,397,511Q). Expression levels of α-ENaC lacking one or all N-glycosylation sites was markedly decreased (55% for N232Q, 35% for N511Q and 34% for N232,293,312,397,511Q compared to WT hENaC, respectively).

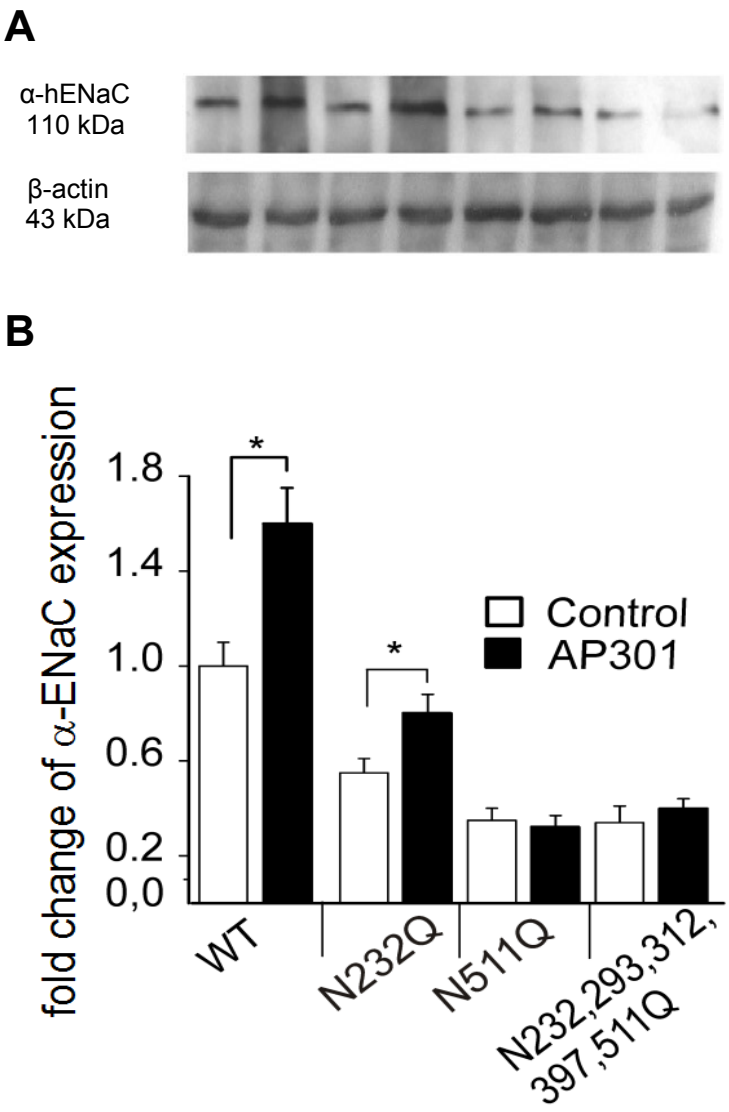

Fig. 17. Increase in expression levels of α-hENaC (~110 kDa) in HEK-293 cells expressing WT α-hENaC or mutants lacking one or all five N-glycosylation sites in the extracellular domain. Cells were treated with 200 nM AP301. β-actin was used as loading control. **A:** One representative image of protein bands is shown. **B:** Increase of α-hENaC expression could only be observed in WT and N232Q mutants. No increase was appreciable in N511Q and α-hENaC lacking all N-glycosylation sites (N232,293,312,397,511Q). Results are shown as mean values ± SEM. p-values were determined by unpaired t-test. Statistical significance was set at $p<0.05$. *$p<0.05$ (n=4-7)

These results suggest an important influence of N-glycosylation in α-hENaC's extracellular domain, especially of residue N511, for the effect of AP301.

4. Discussion

4.1. Effect on endogenous ENaC expression

AP301 has been shown to increase expression of α-ENaC in the epithelial lung cell line H441 (Czikora et al., 2014). The results of the present study suggest a similar effect in A549 and RPMI-2650 cells. The other known pore-forming subunit δ-ENaC shows a comparable response to AP301 in A549 cells. The lack of increased expression in RPMI-2650 cells for δ-ENaC is hard to explain. One reason could be the low number of repeats (n=2) for these experiments. A very minor, insignificant increase in expression could be observed, which might be higher in a larger number of experiments.

When considering the results presented here, one has to keep in mind that Western blotting is only a semi-quantitative technique (Yang and Mahmood, 2012) and is therefore not suited to detect minor changes in protein expression, especially in a low number of experimental repeats. Due to the naturally high variation in biological material (i.e. cell cultures) and the multi-step process required for sample preparation in Western blotting, results tend to have low precision (Koller and Wätzig, 2005). Other major problems include binding of antibodies (Gilda et al., 2015) and densitometric quantification of protein bands (Gassmann et al., 2009). Although experiments in this study were carried out with great care, inaccuracies cannot be excluded and may account for poor statistical significance. Thus, to obtain significant and reliable data a higher number of experimental repeats would have been required to test for an increase in ENaC expression.

Another limitation of this study is the use of whole-cell protein. ENaC is known to be stored in an intracellular pool, from where it can be shifted to the apical membrane (Snyder, 2002; Butterworth et al., 2008; Kellenberger and Schild, 2014). An approach using whole-cell protein, as described here, is therefore unable to distinguish between membrane-bound and pooled ENaC molecules.

Our research group was recently able to resolve these issues by applying biotinylation in order to selectively recover ENaC from apical membranes (Shabbir et al., 2015). The results from this publication show a stronger (up to +70% for δ-ENaC) and statistically significant increase in ENaC expression for α and δ subunits in A549 cells treated with 200 nM AP301 and therefore confirm the find-

ings presented here[1]. Another interesting observation from this study is the apparent lack of effect on expression of β- and γ-ENaC in A549 cells (Shabbir et al., 2015), indicating a selective influence on pore-forming ENaC subunits.

α- and δ-hENaC are expressed in various isoforms in lung epithelial cells (Xu and Chu, 2007; Ji et al., 2012). This study focused on the expression of α_2 and δ_1 isoforms for various reasons: in A549 cells α_2 seems to be the main isoform, whereas α_1 is only expressed in low quantity (see Fig. 7). For δ-hENaC, δ_1 and δ_2 were observed in comparable quantities in A549 cells, showing similar increase in expression when treated with AP301. Fragments of both subunits, probably from proteolytic cleavage, could be observed in this cell line. Quantification of these cleaved products and other isoforms of α- and δ-hENaC was not performed. Based on the intensity of the appreciable proteins bands, a similar effect of AP301 on these proteins might be estimated. However, further experiments would be required to assess a selective effect on different ENaC isoforms or proteolytic fragments by AP301.

Magnitude of whole-cell ion current is determined by the amount of channel expression at the cell surface, single channel current amplitude and open probability (Shabbir et al., 2015). Recent data has suggested an increase of ENaC expression induced by AP301 (Czikora et al., 2014). The results presented here point to a similar effect. Nevertheless, the influence on protein expression was comparatively small — roughly 20% increase compared to control after 5 min — and cannot account for the strong increase (up to 20-fold in A549 cells) in ENaC-mediated Na^+ current observed in whole-cell patch clamp experiments (Hazemi et al., 2010; Shabbir et al., 2013; Tzotzos et al., 2013). Persistent increase in open probability of ENaC (Shabbir et al., 2013) therefore seems to be the main effect of AP301, with transient increase in expression being a secondary effect.

[1] For clarification, the author would like to point out that the results presented in this thesis were gathered before the publication of this paper and should therefore be considered preliminary rather than supplementary.

4.2. Influence of proteolytic activation

This study tried to assess the influence of proteolytic cleavage on the effect that AP301 has on ENaC expression. Human nasal epithelial cells express hENaC mainly in a near-silent conformation and require proteolytic processing for channel activation (Prulière-Escabasse et al., 2010). In the nasal epithelial cell line RPMI-2650, proteolysis has been shown to be a prerequisite for the current-enhancing of AP301 on hENaC (see Fig. 11) (Shabbir et al., 2013).

The results presented here suggest an effect on hENaC expression regardless of proteolytic cleavage of channel proteins.

Experiments conducted in HEK-293 cells using unglycosylated α-hENaC mutants in this study (see. Fig. 17) as well as recent findings from our research group were able to establish the importance of N-glycosylation of asparagine residues in the extracellular domain of α- and δ-ENaC for the increase in channel expression mediated by AP301 (Shabbir et al., 2015). Particularly one N-glycosylated residue of α-hENaC, N511, which is presumed to be located the furthest away from the transmembrane domain and therefore uniquely exposed, has been implicated in being of major importance for binding of AP301 (Shabbir et al., 2015). This glycosylated residue is probably located in the knuckle region of α-ENaC's extracellular domain (Shabbir et al., 2015).

Cleavage sites for proteases in α-ENaC, however, are located in finger domain (Kleyman et al., 2009). The homology model proposed by Kashlan and Kleyman (see Fig. 1) places the inhibitory tract, which is removed by proteolytic processing, at the interface of the thumb and finger domains (Kashlan and Kleyman, 2011). For this reason, it would seem coherent that proteolysis and subsequent removal of a short peptide in a domain distinct from the knuckle region, implicated in binding of AP301, has no substantial influence on the effects mediated by AP301.

On the other hand, based on the homology model the knuckle and the finger/thumb domains are located in relatively close proximity to each other (Kashlan and Kleyman, 2011). Therefore, allosteric inhibition of AP301 binding by the inhibitory tract cannot be excluded. Anyhow, it has to be taken into account that sequence identity in the finger, knuckle and thumb domain is poor between members of the DEG/ENaC superfamily (Kashlan and Kleyman, 2011), making these considerations highly speculative.

Why AP301 would increase channel open probability only in proteolytically cleaved ENaC, as observed in whole-cell patch clamp recordings (Shabbir et al., 2013), whereas channel expression seems to be increased regardless, remains unclear.

Czikora et al. have recently proposed a mechanism of action for the TIP peptide, which consists of stabilization of a complex formed by ENaC, PIP_2 and a protein called MARCKS that is crucial for the open conformation of the channel (Czikora et al., 2014). The authors reasoned that this stabilization also prevents PIP_2-mediated generation of diacylglycerol by phospholipase C and subsequent activation of protein kinase C, a process responsible for decreased expression of α-ENaC (Czikora et al., 2014). However, such a mechanism would require binding of AP301 to ENaC for increased open probability as well as increased expression, making a separation of those two effects in uncleaved ENaC proteins, as found in RPMI-2650 cells, unlikely.

Due to the speculative nature of the results from RPMI-2650 cells in this study, it is impossible to come to a meaningful conclusion. Further investigation will therefore be required to resolve this issue.

4.3. Importance of N-glycosylation in α-ENaC

As described above, glycosylated residues in the extracellular domain of ENaC have been implicated in the binding of AP301 (Czikora et al., 2014). Previous studies have also demonstrated a lack of efficacy of AP301 on deglycosylated hENaC proteins, treated with PNGase F to remove N-linked glycans, in A549 and H441 cells as well as HEK-293 cells expressing hENaC heterologously (Shabbir et al., 2013; Czikora et al., 2014).

Lectins are proteins that are highly specific for recognition of sugar moieties (Sharon, 2004). The lectin-like domain of TNF-α is therefore expected to bind certain sugars. This was recently demonstrated in a molecular docking and dynamics simulation study, which proposed the binding of TNF-α to N,N'-diacetylchitobiose via its lectin-like domain (Dulebo et al., 2012).

Thus, the present study tried to analyse the effect of AP301 on channel expression in HEK-293 cells expressing either wild type α-hENaC or mutated proteins lacking one or all glycosylated asparagine residues in the extracellular domain of the channel.

Unglycosylated α-hENaC mutants lacking either N511 or all five N-glycosylation sites (N232,293,312,397,511Q) did not respond to AP301 treatment with an increase in expression. In contrast, a strong and significant effect could be observed in WT α-hENaC as well as N232Q mutants, albeit the latter showed a weaker increase.

The stark difference between N232Q and N511Q mutants will require further investigation. A possible explanation could be the exposed location of the N511 residue, as predicted by the homology model of Kashlan and Kleyman mentioned above (Kashlan and Kleyman, 2011). Higher exposure of N511, compared to other N-glycosylated residues, might account for a preferential binding of AP301 to this position (Shabbir et al., 2015).

These results emphasise the importance of N-glycosylation of residues in the extracellular domain of α-hENaC for the effect of AP301 on channel expression. Our research group has recently demonstrated a similar response for the other known pore-forming subunit, δ-hENaC (Shabbir et al., 2015).

Other experiments conducted in A549 cells have had a matching outcome: removal of N-glycans with PNGase F blunted the effect of AP301 on hENaC expression (data not shown).

It is essential to note that the importance of N-glycosylation for ion channel function is still a matter of debate (Shabbir et al., 2015). However, our research group and others found no effect of N-deglycosylation on electrophysiological properties of hENaC (Snyder et al., 1994; Shabbir et al., 2015).

4.4. Conclusion

To summarise, this study proposes that the novel lung edema therapeutic AP301 has a minor effect on protein expression of the pore-forming subunits α- and δ-hENaC *in vitro*. Western blot experiments using two cell lines, namely A549 and RPMI-2650, which express hENaC endogenously, were performed.

An increase in expression of roughly 20% for both subunits was observed in A549 cells. α-hENaC was expressed in slightly higher quantities in RPMI-2650 cells treated with AP301 compared to control, whereas δ-hENaC showed no increase. However, this results were inconclusive due to low statistical significance.

Observations in HEK-293 cells expressing either partly or completely unglycosylated α-hENaC, co-expressed with β and γ subunits, suggest that N-glycans in the extracellular domain of ENaC play a pivotal role for the effect of AP301 on the channel. Partly unglycosylated α-hENaC in position N511 or completely unglycosylated α subunits did not elicit a response to AP301.

5. References

Althaus, M., Clauss, W.G., Fronius, M., 2011. Amiloride-Sensitive Sodium Channels and Pulmonary Edema. Pulm. Med. 2011, 1–8. doi:10.1155/2011/830320

Anantharam, A., Tian, Y., Palmer, L.G., 2006. Open probability of the epithelial sodium channel is regulated by intracellular sodium: Intracellular Na + regulates epithelial Na + channel kinetics. J. Physiol. 574, 333–347. doi:10.1113/jphysiol.2006.109173

APEPTICO - Innovation in peptide drugs - Vienna, Austria [WWW Document], 2015. URL http://www.apeptico.com/index-home (accessed 5.11.15).

Baconguis, I., Bohlen, C.J., Goehring, A., Julius, D., Gouaux, E., 2014. X-Ray Structure of Acid-Sensing Ion Channel 1–Snake Toxin Complex Reveals Open State of a Na+-Selective Channel. Cell 156, 717–729. doi:10.1016/j.cell.2014.01.011

Bangel, N., Dahlhoff, C., Sobczak, K., Weber, W.-M., Kusche-Vihrog, K., 2008. Upregulated expression of ENaC in human CF nasal epithelium. J. Cyst. Fibros. 7, 197–205. doi:10.1016/j.jcf.2007.07.012

Bangel-Ruland, N., Sobczak, K., Christmann, T., Kentrup, D., Langhorst, H., Kusche-Vihrog, K., Weber, W.-M., 2010. Characterization of the Epithelial Sodium Channel δ-Subunit in Human Nasal Epithelium. Am. J. Respir. Cell Mol. Biol. 42, 498–505. doi:10.1165/rcmb.2009-0053OC

Bassford, C.R., Thickett, D.R., Perkins, G.D., 2012. The rise and fall of β-agonists in the treatment of ARDS. Crit Care 16, 208.

Berthiaume, Y., Matthay, M.A., 2007. Alveolar edema fluid clearance and acute lung injury. Respir. Physiol. Neurobiol. 159, 350–359. doi:10.1016/j.resp.2007.05.010

Bize, V., Horisberger, J.-D., 2007. Sodium self-inhibition of human epithelial sodium channel: selectivity and affinity of the extracellular sodium sensing site. AJP Ren. Physiol. 293, F1137–F1146. doi:10.1152/ajprenal.00100.2007

Börjesson, A., Norlin, A., Wang, X., Andersson, R., Folkesson, H.G., 2000. TNF-α stimulates alveolar liquid clearance during intestinal ischemia-reperfusion in rats. Am. J. Physiol.-Lung Cell. Mol. Physiol. 278, L3–L12.

Braun, C., Hamacher, J., Morel, D.R., Wendel, A., Lucas, R., 2005. Dichotomal role of TNF in experimental pulmonary edema reabsorption. J. Immunol. 175, 3402–3408.

Bruns, J.B., Carattino, M.D., Sheng, S., Maarouf, A.B., Weisz, O.A., Pilewski, J.M., Hughey, R.P., Kleyman, T.R., 2006. Epithelial Na+ Channels Are Fully Activated by Furin- and Prostasin-dependent Release of an Inhibitory Peptide from the gamma-Subunit. J. Biol. Chem. 282, 6153–6160. doi:10.1074/jbc.M610636200

Butterworth, M.B., Edinger, R.S., Frizzell, R.A., Johnson, J.P., 2008. Regulation of the epithelial sodium channel by membrane trafficking. AJP Ren. Physiol. 296, F10–F24. doi:10.1152/ajprenal.90248.2008

Caldwell, R.A., 2003. Serine protease activation of near-silent epithelial Na+ channels. AJP Cell Physiol. 286, 190C–194. doi:10.1152/ajpcell.00342.2003

Canessa, C.M., Merillat, A.M., Rossier, B.C., 1994a. Membrane topology of the epithelial sodium channel in intact cells. Am. J. Physiol. 267, C1682–1690.

Canessa, C.M., Schild, L., Buell, G., Thorens, B., Gautschi, I., Horisberger, J.D., Rossier, B.C., 1994b. Amiloride-sensitive epithelial Na+ channel is made of three homologous subunits. Nature 367, 463–467. doi:10.1038/367463a0

Carattino, M.D., Sheng, S., Bruns, J.B., Pilewski, J.M., Hughey, R.P., Kleyman, T.R., 2006. The Epithelial Na+ Channel Is Inhibited by a Peptide Derived from Proteolytic Processing of Its alpha Subunit. J. Biol. Chem. 281, 18901–18907. doi:10.1074/jbc.M604109200

Chraïbi, A., Vallet, V., Firsov, D., Hess, S.K., Horisberger, J.-D., 1998. Protease modulation of the activity of the epithelial sodium channel expressed in Xenopus oocytes. J. Gen. Physiol. 111, 127–138.

Cleland, J.G., Yassin, A.S., Khadjooi, K., 2010. Acute heart failure: focusing on acute cardiogenic pulmonary oedema. Clin. Med. 10, 59–64.

Collier, D.M., Snyder, P.M., 2009a. Extracellular Protons Regulate Human ENaC by Modulating Na+ Self-inhibition. J. Biol. Chem. 284, 792–798. doi:10.1074/jbc.M806954200

Collier, D.M., Snyder, P.M., 2009b. Extracellular Chloride Regulates the Epithelial Sodium Channel. J. Biol. Chem. 284, 29320–29325. doi:10.1074/jbc.M109.046771

Czikora, I., Alli, A., Bao, H.-F., Kaftan, D., Sridhar, S., Apell, H.-J., Gorshkov, B., White, R., Zimmermann, A., Wendel, A., Pauly-Evers, M., Hamacher, J., Garcia-Gabay, I., Fischer, B., Verin, A., Bagi, Z., Pittet, J.F., Shabbir, W., Lemmens-Gruber, R., Chakraborty, T., Lazrak, A., Matthay, M.A., Eaton, D.C., Lucas, R., 2014. A novel tumor necrosis factor-mediated mechanism of direct epithelial sodium channel activation. Am. J. Respir. Crit. Care Med. 190, 522–532. doi:10.1164/rccm.201405-0833OC

Dagenais, A., 2004. Downregulation of ENaC activity and expression by TNF-α in alveolar epithelial cells. AJP Lung Cell. Mol. Physiol. 286, 301L–311. doi:10.1152/ajplung.00326.2002

Dulebo, A., Ettrich, R., Lucas, R., Kaftan, D., 2012. A computational study of the oligosaccharide binding sites in the lectin-like domain of Tumor Necrosis Factor and the TNF-derived TIP peptide. Curr. Pharm. Des. 18, 4236–4243.

Eaton, D.C., Helms, M.N., Koval, M., Bao, H.F., Jain, L., 2009. The Contribution of Epithelial Sodium Channels to Alveolar Function in Health and Disease. Annu. Rev. Physiol. 71, 403–423. doi:10.1146/annurev.physiol.010908.163250

Elia, N., Tapponnier, M., Matthay, M.A., Hamacher, J., Pache, J.-C., Bründler, M.-A., Totsch, M., De Baetselier, P., Fransen, L., Fukuda, N., Morel, D.R., Lucas, R., 2003. Functional Identification of the Alveolar Edema Reabsorption Activity of Murine Tumor Necrosis Factor-α. Am. J. Respir. Crit. Care Med. 168, 1043–1050. doi:10.1164/rccm.200206-618OC

Eskandari, S., Snyder, P.M., Kreman, M., Zampighi, G.A., Welsh, M.J., Wright, E.M., 1999. Number of subunits comprising the epithelial sodium channel. J. Biol. Chem. 274, 27281–27286.

Firsov, D., Gautschi, I., Merillat, A.-M., Rossier, B.C., Schild, L., 1998. The heterotetrameric architecture of the epithelial sodium channel (ENaC). EMBO J. 17, 344–352.

Firsov, D., Schild, L., Gautschi, I., Mérillat, A.-M., Schneeberger, E., Rossier, B.C., 1996. Cell surface expression of the epithelial Na channel and a mutant causing Liddle syndrome: a quantitative approach. Proc. Natl. Acad. Sci. 93, 15370–15375.

Fischer, B., 2015. APEPTICO, press release. [WWW Document]. URL http://www.apeptico.com/self_service_lite/content/index/-sub-/news/files/press_release_apeptico_2015_06_01_5577e59107fbe.pdf. Available from: <http://www.apeptico.com/index-news> (accessed 4.11.15).

Folkesson, H.G., Matthay, M.A., 2006. Alveolar epithelial ion and fluid transport: recent progress. Am. J. Respir. Cell Mol. Biol. 35, 10–19.

Fukuda, N., Jayr, C., Lazrak, A., Wang, Y., Lucas, R., Matalon, S., Matthay, M.A., 2001. Mechanisms of TNF-α stimulation of amiloride-sensitive sodium transport across alveolar epithelium. Am. J. Physiol.-Lung Cell. Mol. Physiol. 280, L1258–L1265.

Garcia-Caballero, A., Dang, Y., He, H., Stutts, M.J., 2008. ENaC Proteolytic Regulation by Channel-activating Protease 2. J. Gen. Physiol. 132, 521–535. doi:10.1085/jgp.200810030

Garty, H., 1994. Molecular properties of epithelial, amiloride-blockable Na+ channels. FASEB J. 8, 522–528.

Gassmann, M., Grenacher, B., Rohde, B., Vogel, J., 2009. Quantifying Western blots: Pitfalls of densitometry. ELECTROPHORESIS 30, 1845–1855. doi:10.1002/elps.200800720

Gilda, J.E., Ghosh, R., Cheah, J.X., West, T.M., Bodine, S.C., Gomes, A.V., 2015. Western Blotting Inaccuracies with Unverified Antibodies: Need for a Western Blotting Minimal Reporting Standard (WBMRS). PLOS ONE 10, e0135392. doi:10.1371/journal.pone.0135392

Gunthorpe, M.J., Smith, G.D., Davis, J.B., Randall, A.D., 2001. Characterisation of a human acid-sensing ion channel (hASIC1a) endogenously expressed in HEK293 cells. Pflüg. Arch. Eur. J. Physiol. 442, 668–674.

Haerteis, S., Krueger, B., Korbmacher, C., Rauh, R., 2009. The delta-Subunit of the Epithelial Sodium Channel (ENaC) Enhances Channel Activity and Alters Proteolytic ENaC Activation. J. Biol. Chem. 284, 29024–29040. doi:10.1074/jbc.M109.018945

Hasanovic, M., 2013. Interaction of TNF-α derived peptide with Epithelial Sodium Channel, Bachelor thesis, IMC Fachhochschule Krems (University of Applied Sciences)

Hazemi, P., Tzotzos, S.J., Fischer, B., Andavan, G.S.B., Fischer, H., Pietschmann, H., Lucas, R., Lemmens-Gruber, R., 2010. Essential Structural Features of TNF-α Lectin-like Domain Derived Peptides for Activation of Amiloride-Sensitive Sodium Current in A549 Cells. J. Med. Chem. 53, 8021–8029. doi:10.1021/jm100767p

Horisberger, J.-D., Chraïbi, A., 2004. Epithelial sodium channel: a ligand-gated channel? Nephron Physiol. 96, p37–41. doi:10.1159/000076406

Hummler, E., Barker, P., Gatzy, J., Beermann, F., Verdumo, C., Schmidt, A., Boucher, R., Rossier, B.C., 1996. Early death due to defective neonatal lung liquid clearance in alpha-ENaC-deficient mice. Nat. Genet. 12, 325–328. doi:10.1038/ng0396-325

Jasti, J., Furukawa, H., Gonzales, E.B., Gouaux, E., 2007. Structure of acid-sensing ion channel 1 at 1.9 Å resolution and low pH. Nature 449, 316–323. doi:10.1038/nature06163

Jiang, Y., Xu, J., Chen, Y., Shi, J., Zhang, C., Li, J., 2015. Expression and distribution of epithelial sodium channel in nasal polyp and nasal mucosa. Eur. Arch. Otorhinolaryngol. 272, 3361–3366. doi:10.1007/s00405-014-3477-5

Ji, H.-L., Su, X.-F., Kedar, S., Li, J., Barbry, P., Smith, P.R., Matalon, S., Benos, D.J., 2006. δ-Subunit Confers Novel Biophysical Features to αβγ-Human Epithelial Sodium Channel (ENaC) via a Physical Interaction. J. Biol. Chem. 281, 8233–8241. doi:10.1074/jbc.M512293200

Ji, H.-L., Zhao, R.-Z., Chen, Z.-X., Shetty, S., Idell, S., Matalon, S., 2012. δ ENaC: a novel divergent amiloride-inhibitable sodium channel. AJP Lung Cell. Mol. Physiol. 303, L1013–L1026. doi:10.1152/ajplung.00206.2012

Johnson, E.R., Matthay, M.A., 2010. Acute lung injury: epidemiology, pathogenesis, and treatment. J. Aerosol Med. Pulm. Drug Deliv. 23, 243–252.

Kashlan, O.B., Adelman, J.L., Okumura, S., Blobner, B.M., Zuzek, Z., Hughey, R.P., Kleyman, T.R., Grabe, M., 2011. Constraint-based, Homology Model of the Extracellular Domain of the Epithelial Na+ Channel Subunit Reveals a Mechanism of Channel Activation by Proteases. J. Biol. Chem. 286, 649–660. doi:10.1074/jbc.M110.167098

Kashlan, O.B., Kleyman, T.R., 2011. ENaC structure and function in the wake of a resolved structure of a family member. AJP Ren. Physiol. 301, F684–F696. doi:10.1152/ajprenal.00259.2011

Kellenberger, S., Schild, L., 2014. International Union of Basic and Clinical Pharmacology. XCI. Structure, Function, and Pharmacology of Acid-Sensing Ion Channels and the Epithelial Na+ Channel. Pharmacol. Rev. 67, 1–35. doi:10.1124/pr.114.009225

Kleyman, T.R., Carattino, M.D., Hughey, R.P., 2009. ENaC at the Cutting Edge: Regulation of Epithelial Sodium Channels by Proteases. J. Biol. Chem. 284, 20447–20451. doi:10.1074/jbc.R800083200

Koller, A., Wätzig, H., 2005. Precision and variance components in quantitative gel electrophoresis. ELECTROPHORESIS 26, 2470–2475. doi:10.1002/elps.200500024

Kosari, F., Sheng, S., Li, J., Mak, D.-O.D., Foskett, J.K., Kleyman, T.R., 1998. Subunit stoichiometry of the epithelial sodium channel. J. Biol. Chem. 273, 13469–13474.

Lazrak, A., Samanta, A., Matalon, S., 2000. Biophysical properties and molecular characterization of amiloride-sensitive sodium channels in A549 cells. Am. J. Physiol.-Lung Cell. Mol. Physiol. 278, L848–L857.

Lucas, R., Lou, J., Morel, D.R., Ricou, B., Suter, P.M., Grau, G.E., 1997. TNF receptors in the microvascular pathology of acute respiratory distress syndrome and cerebral malaria. J. Leukoc. Biol. 61, 551–558.

Mano, I., Driscoll, M., 1999. DEG/ENaC channels: a touchy superfamily that watches its salt. BioEssays News Rev. Mol. Cell. Dev. Biol. 21, 568–578. doi:10.1002/(SICI)1521-1878(199907)21:7<568::AID-BIES5>3.0.CO;2-L

Mascher, D., Tscherwenka, W., Mascher, H., Fischer, B., 2012. Sensitive determination of the peptide AP301 – A motif of TNF-α – From human plasma using HPLC–MS/MS. J. Chromatogr. B 908, 18–22. doi:10.1016/j.jchromb.2012.09.028

Matthay, M.A., 2014. Resolution of Pulmonary Edema. Thirty Years of Progress. Am. J. Respir. Crit. Care Med. 189, 1301–1308. doi:10.1164/rccm.201403-0535OE

Matthay, M.A., Folkesson, H.G., Clerici, C., 2002. Lung Epithelial Fluid Transport and the Resolution of Pulmonary Edema. Physiol. Rev. 82, 569–600. doi:10.1152/physrev.00003.2002

McDonald, F.J., Price, M.P., Snyder, P.M., Welsh, M.J., 1995. Cloning and expression of the beta- and gamma-subunits of the human epithelial sodium channel. Am. J. Physiol. 268, C1157–1163.

Morimoto, T., 2006. Mechanism underlying flow stimulation of sodium absorption in the mammalian collecting duct. AJP Ren. Physiol. 291, F663–F669. doi:10.1152/ajprenal.00514.2005

Murray, J.F., 2011. Pulmonary edema: pathophysiology and diagnosis. Int. J. Tuberc. Lung Dis. 15, 155–160.

Palmer, L.G., 1987. Ion selectivity of epithelial Na channels. J. Membr. Biol. 96, 97–106.

Palmer, L.G., Frindt, G., 1986. Amiloride-sensitive Na channels from the apical membrane of the rat cortical collecting tubule. Proc. Natl. Acad. Sci. 83, 2767–2770.

Palmer, L.G., Patel, A., Frindt, G., 2012. Regulation and dysregulation of epithelial Na+ channels. Clin. Exp. Nephrol. 16, 35–43. doi:10.1007/s10157-011-0496-z

Prince, L.S., Welsh, M.J., 1998. Cell surface expression and biosynthesis of epithelial Na+ channels. Biochem. J. 336 (Pt 3), 705–710.

Prulière-Escabasse, V., Clerici, C., Vuagniaux, G., Coste, A., Escudier, E., Planès, C., others, 2010. Effect of neutrophil elastase and its inhibitor EPI-hNE4 on transepithelial sodium transport across normal and cystic fibrosis human nasal epithelial cells. Respir. Res 11, 141.

Renard, S., Lingueglia, E., Voilley, N., Lazdunski, M., Barbry, P., 1994. Biochemical analysis of the membrane topology of the amiloride-sensitive Na+ channel. J. Biol. Chem. 269, 12981–12986.

Rezaiguia, S., Garat, C., Delclaux, C., Meignan, M., Fleury, J., Legrand, P., Matthay, M.A., Jayr, C., 1997. Acute bacterial pneumonia in rats increases alveolar epithelial fluid clearance by a tumor necrosis factor-alpha-dependent mechanism. J. Clin. Invest. 99, 325–335. doi:10.1172/JCI119161

Rossier, B.C., Pradervand, S., Schild, L., Hummler, E., 2002. Epithelial sodium channel and the control of sodium balance: interaction between genetic and environmental factors. Annu. Rev. Physiol. 64, 877–897. doi:10.1146/annurev.physiol.64.082101.143243

Ruffieux-Daidie, D., Poirot, O., Boulkroun, S., Verrey, F., Kellenberger, S., Staub, O., 2008. Deubiquitylation Regulates Activation and Proteolytic Cleavage of ENaC. J. Am. Soc. Nephrol. 19, 2170–2180. doi:10.1681/ASN.2007101130

Schild, L., 2010. The epithelial sodium channel and the control of sodium balance. Biochim. Biophys. Acta BBA - Mol. Basis Dis. 1802, 1159–1165. doi:10.1016/j.bbadis.2010.06.014

Schild, L., Schneeberger, E., Gautschi, I., Firsov, D., 1997. Identification of amino acid residues in the α, β, and γ subunits of the epithelial sodium channel (ENaC) involved in amiloride block and ion permeation. J. Gen. Physiol. 109, 15–26.

Shabbir, W., Scherbaum-Hazemi, P., Tzotzos, S., Fischer, B., Fischer, H., Pietschmann, H., Lucas, R., Lemmens-Gruber, R., 2013. Mechanism of Action of Novel Lung Edema Therapeutic AP301 by Activation of the Epithelial Sodium Channel. Mol. Pharmacol. 84, 899–910. doi:10.1124/mol.113.089409

Shabbir, W., Tzotzos, S., Bedak, M., Aufy, M., Willam, A., Kraihammer, M., Holzner, A., Czikora, I., Scherbaum-Hazemi, P., Fischer, H., Pietschmann, H., Fischer, B., Lucas, R., Lemmens-Gruber, R., 2015. Glycosylation-dependent activation of epithelial sodium channel by solnatide. Biochem. Pharmacol. doi:10.1016/j.bcp.2015.08.003

Sharon, N., 2004. History of lectins: from hemagglutinins to biological recognition molecules. Glycobiology 14, 53R–62R. doi:10.1093/glycob/cwh122

Snyder, P.M., 2005. Minireview: Regulation of Epithelial Na+ Channel Trafficking. Endocrinology 146, 5079–5085. doi:10.1210/en.2005-0894

Snyder, P.M., 2002. The epithelial Na+ channel: cell surface insertion and retrieval in Na+ homeostasis and hypertension. Endocr. Rev. 23, 258–275.

Snyder, P.M., Cheng, C., Prince, L.S., Rogers, J.C., Welsh, M.J., 1998. Electrophysiological and biochemical evidence that DEG/ENaC cation channels are composed of nine subunits. J. Biol. Chem. 273, 681–684.

Snyder, P.M., McDonald, F.J., Stokes, J.B., Welsh, M.J., 1994. Membrane topology of the amiloride-sensitive epithelial sodium channel. J. Biol. Chem. 269, 24379–24383.

Staruschenko, A., Adams, E., Booth, R.E., Stockand, J.D., 2005. Epithelial Na+ Channel Subunit Stoichiometry. Biophys. J. 88, 3966–3975. doi:10.1529/biophysj.104.056804

Staruschenko, A., Medina, J.L., Patel, P., Shapiro, M.S., Booth, R.E., Stockand, J.D., 2004. Fluorescence Resonance Energy Transfer Analysis of Subunit Stoichiometry of the Epithelial Na+ Channel. J. Biol. Chem. 279, 27729–27734. doi:10.1074/jbc.M404169200

Stewart, A.P., Haerteis, S., Diakov, A., Korbmacher, C., Edwardson, J.M., 2011. Atomic Force Microscopy Reveals the Architecture of the Epithelial Sodium Channel (ENaC). J. Biol. Chem. 286, 31944–31952. doi:10.1074/jbc.M111.275289

Thomas, C.P., Auerbach, S., Stokes, J.B., Volk, K.A., 1998. 5' heterogeneity in epithelial sodium channel alpha-subunit mRNA leads to distinct NH2-terminal variant proteins. Am. J. Physiol. 274, C1312–1323.

Tzotzos, S., Fischer, B., Fischer, H., Pietschmann, H., Lucas, R., Dupré, G., Lemmens-Gruber, R., Hazemi, P., Prymaka, V., Shabbir, W., 2013. AP301, a synthetic peptide mimicking the lectin-like domain of TNF, enhances amiloride-sensitive Na+ current in primary dog, pig and rat alveolar type II cells. Pulm. Pharmacol. Ther. 26, 356–363. doi:10.1016/j.pupt.2012.12.011

Valentijn, J.A., Fyfe, G.K., Canessa, C.M., 1998. Biosynthesis and Processing of Epithelial Sodium Channels in Xenopus Oocytes. J. Biol. Chem. 273, 30344–30351.

Vallet, V., Chraibi, A., Gaeggeler, H.P., Horisberger, J.D., Rossier, B.C., 1997. An epithelial serine protease activates the amiloride-sensitive sodium channel. Nature 389, 607–610. doi:10.1038/39329

Waldmann, R., Champigny, G., Bassilana, F., Voilley, N., Lazdunski, M., 1995. Molecular cloning and functional expression of a novel amiloride-sensitive Na+ channel. J. Biol. Chem. 270, 27411–27414.

Ware, L.B., Matthay, M.A., 2001. Alveolar fluid clearance is impaired in the majority of patients with acute lung injury and the acute respiratory distress syndrome. Am. J. Respir. Crit. Care Med. 163, 1376–1383.

Wemmie, J.A., Taugher, R.J., Kreple, C.J., 2013. Acid-sensing ion channels in pain and disease. Nat. Rev. Neurosci. 14, 461–471. doi:10.1038/nrn3529

Xu, H., Chu, S., 2007. ENaC α-subunit variants are expressed in lung epithelial cells and are suppressed by oxidative stress. AJP Lung Cell. Mol. Physiol. 293, L1454–L1462. doi:10.1152/ajplung.00248.2007

Yamagata, T., Yamagata, Y., Nishimoto, T., Hirano, T., Nakanishi, M., Minakata, Y., Ichinose, M., Dagenais, A., Berthiaume, Y., 2009. The regulation of amiloride-sensitive epithelial sodium channels by tumor necrosis factor-alpha in injured lungs and alveolar type II cells. Respir. Physiol. Neurobiol. 166, 16–23. doi:10.1016/j.resp.2008.12.008

Yang, P.-C., Mahmood, T., 2012. Western blot: Technique, theory, and trouble shooting. North Am. J. Med. Sci. 4, 429. doi:10.4103/1947-2714.100998

Zhao, R.-Z., Nie, H.-G., Su, X.-F., Han, D.-Y., Lee, A., Huang, Y., Chang, Y., Matalon, S., Ji, H.-L., 2012. Characterization of a novel splice variant of δ ENaC subunit in human lungs. AJP Lung Cell. Mol. Physiol. 302, L1262–L1272. doi:10.1152/ajplung.00331.2011

6. Curriculum vitae

Personal details

Name	Martin Kraihammer
Date of birth	April 9th, 1990
Place of birth	Salzburg, Austria
Citizenship	Austrian
Principal residence	Teybergasse 14/9 A-1140 Vienna
Secondary residence	Irlachring 3 A-5201 Seekirchen am Wallersee
Phone number	+43 650 4175552
E-mail	martin.kraihammer@gmail.com

Education

since 01/10/2009	Pharmacy studies at the University of Vienna Diploma thesis at the Department of Pharmacology and Toxicology: "*The Effect of AP301 on the expression of α- and δ-ENaC in A549 and RPMI-2650 cells*" Supervisor: Prof. Dr. Rosa Lemmens-Gruber
08/2015	Co-author of the publication: Shabbir W, Tzotzos S, Bedak M, Aufy M, Willam A, Kraihammer M, Holzner A, Czikora I, Scherbaum-Hazemi P, Fischer H, Pietschmann H, Fischer B, Lucas R, Lemmens-Gruber R "*Glycosylation-dependent activation of epithelial sodium channel by solnatide*" Biochem Pharmacol. 2015 Aug 5. doi: 10.1016/j.bcp.2015.08.003.
10/2012 - 06/2015	Tutor at the University of Vienna, Department of Pharmacology and Toxicology

2000 - 2008	Secondary School Seekirchen, Austria School leaving examination with distinction in the following subjects: German, Mathematics, English, Latin, Physics, Chemistry
1996 - 2000	Elementary School Seekirchen, Austria

Work experience

07/2012 – 08/2012	4-week internship at the “Tassilo” pharmacy in Mattsee, Salzburg, Austria
07/2011 – 08/2011	7-week internship at the hospital pharmacy Salzburg, Austria
08/2010 - 09/2010	6-week internship at the hospital pharmacy Salzburg, Austria
10/2008 - 08/2009	Alternative Civilian Service Austrian Red Cross (Tamsweg, Salzburg)

Additional skills

Languages	German – mother tongue English – fluent (First Certificate in English) French – element Latin – element
IT	MS Office (Word, PowerPoint, Excel) European Computer Driving Licence Core